JOURNAL OF GUIDANCE, CONTROL, AND DYNAMICS
Vol. 26, No. 6, November–December 2003

Longitudinal Flight-Path Control Using Online Function Approximation

Jay A. Farrell*
University of California, Riverside, California 92506
Manu Sharma†
Barron Associates, Inc., Charlottesville, Virginia 22901
and
Marios Polycarpou‡
University of Cincinatti, Cincinatti, Ohio 45221-0030

Stable online approximation-based control algorithms are derived for aircraft longitudinal dynamics (γ, α, Q, and V) on an unmanned combat aircraft. The objectives of the control approach are to stabilize the aircraft dynamics and to achieve accurate command tracking in the presence of significant nonlinear model error. This error could be due to mismatch between the true aircraft dynamics and the model available at the control design stage, or could be the result of events that occur during the vehicle flight, that is, battle damage. Lyapunov-type stability analysis and simulation demonstrations of the achieved performance are included.

Nomenclature

$C_D(\boldsymbol{x}_r)$	=	coefficient of drag
$C_{D_{\delta_i}}(\boldsymbol{x}_r)$	=	coefficient of drag due to deflection of surface i
$C_L(\boldsymbol{x}_r)$	=	coefficient of lift
$C_{L_\alpha}(\boldsymbol{x}_r)$	=	coefficient of lift with respect to α
$C_{M_o}(\boldsymbol{x}_r)$	=	coefficient of pitch moment
$C_{M_Q}(\boldsymbol{x}_r)$	=	coefficient of pitch moment due to Q
$C_{M_{\delta_i}}(\boldsymbol{x}_r)$	=	coefficient of pitch moment due to deflection of surface i
c_i, $i \in [1, 9]$	=	inertial parameters; see Ref. 34, p. 80
$\bar{c}$	=	mean aerodynamic chord
$D(\boldsymbol{x})$	=	drag force function
$\hat{D}(\boldsymbol{x}_r)$	=	approximated drag force function
g	=	gravity
K_Q	=	control parameter for Q loop
K_α	=	control parameter for α loop
K_γ	=	control parameter for γ loop
$L(\boldsymbol{x})$	=	lift force function
$\hat{L}(\boldsymbol{x}_r)$	=	approximated lift force function
M	=	Mach number
$\bar{M}(\boldsymbol{x})$	=	pitch moment function
$\hat{M}(\boldsymbol{x}_r)$	=	approximated pitch moment function
P_z	=	matrix used in the inner-loop Lyapunov analysis
Q	=	pitch rate
Q_c	=	commanded pitch rate
$\tilde{Q}$	=	pitch rate tracking error, $Q - Q_c$
$\bar{q}$	=	dynamic pressure, $\frac{1}{2}\rho V^2$
S	=	reference area
T	=	thrust
V	=	airspeed
V_c	=	commanded airspeed
$\tilde{V}$	=	airspeed tracking error, $V - V_c$
$\boldsymbol{x}$	=	vehicle state vector
$\boldsymbol{x}_r$	=	reduced state vector containing only the dominant elements
α	=	angle of attack
α_c	=	commanded angle of attack
$\tilde{\alpha}$	=	angle of attack tracking error, $\alpha - \alpha_c$
γ	=	flight-path angle
γ_c	=	commanded flight-path angle
$\tilde{\gamma}$	=	flight-path angle tracking error, $\gamma - \gamma_c$
$\boldsymbol{\delta}^T$	=	vector of control surface deflections, $[\delta_1, \ldots, \delta_m]$
θ	=	pitch angle
$\bar{\lambda}(P_x)$, $\underline{\lambda}(P_x)$	=	maximum and minimum eigenvalues of P_x
ρ	=	air density
$\phi(\boldsymbol{x}_r)$	=	regressor vector

I. Introduction

THE past few decades have witnessed the development of a number of nonlinear control methodologies for application to advanced flight vehicles. These methods offer both increases in performance as well as reduced development times by dealing with the complete dynamics of the vehicle rather than point designs. Feedback linearization, in its various forms, is perhaps the most commonly employed nonlinear control method in this arena.[1–6] In addition to feedback linearization, other nonlinear methods have also been investigated for flight control. In Ref. 7 a nonlinear model predictive control approach is presented that relies on a Taylor series approximation to the system's differential equations. Optimal control techniques are applied to control load factor in Ref. 8. Prelinearization theory and singular perturbation theory are applied for the derivation of inner and outer loop controllers in Ref. 4.

The main drawback to the mentioned nonlinear control approaches is that, as model-based control methods, they require accurate knowledge of the plant dynamics. This is of significance in flight control because aerodynamic parameters always contain some degree of uncertainty. Although some of these approaches are robust to small modeling errors, they are not intended to accommodate significant unanticipated errors that can occur in the event of failure or battle damage. In such an event, the aerodynamics can change rapidly and deviate significantly from the model used for control design. Uninhabited air vehicles are particularly susceptible to such events because there is no pilot onboard.

Various direct and indirect adaptive approaches have been proposed to address circumstances in which significant modeling error

Received 31 October 2002; revision received 1 February 2003; accepted for publication 25 April 2003.

*Professor, Department of Electrical Engineering.
†Research Engineer, 1160 Pepsi Place, Suite 300. Member AIAA.
‡Professor, Department of Electrical and Computer Engineering.

is present.[9–15] Indirect methods based on modified sequential least squares and model predictive methods[9] were successfully demonstrated in-flight on the VISTA F-16. However, proofs of stability for these indirect linear adaptive controllers have not been presented. Adaptive backstepping-type approaches, in which the linearized aircraft model parameters are estimated online, have also been explored for flight control.[11,12] These methods allow a total stability analysis, but do not provide an easy means of designing the transient response.[12] In addition, because the approach is based on estimated linearized aircraft model parameters, changes in operating point can generate significant tracking error transients while the new linearized model parameters are being estimated. Direct adaptive control has also been successfully demonstrated in flight.[13–16] This approach constructs a dynamic inversion controller for the known aircraft dynamics and then augments this with a neural network to cancel inversion error that arises as a result of model error; no attempt at approximating the nonlinear model is made.

A recent series of articles[12,17–19] discusses and compares various modern control approaches, that is, fuzzy logic, neural, adaptive backstepping, indirect adaptive, nonlinear predictive, gain scheduled dynamic inversion, and variable structure, in a high-fidelity aircraft simulation. The motivation for these articles is that nonlinear controllers have performed well on simplified models but often fail in high-fidelity simulations. In addition, the authors wished to glean the implementation and tuning issues associated with the various methods. Challenges include actuator nonlinearities, loop interactions, incorporation of pilot feedback, configuration changes, and controller validation. Specific conclusions of Ref. 12 are that the backstepping and indirect adaptive approaches achieved the best performance for a reasonable amount of design effort, that the Lyapunov stability results that are possible with the backstepping approach are beneficial, that the backstepping approach yields faster convergence than the indirect adaptive approach, that in the backstepping approach it was more difficult to select the design parameters to specify the transient response, and that the backstepping approach required larger actuator response.

This work presents a flight-control approach that is based on ideas from feedback linearization and backstepping.[20–22] The control law incorporates online function approximators to estimate aerodynamic force and moment functions. The theory for approximation-based nonlinear control that is used is provided in Refs. 23–28. The main advantages of this approach include a controller with a small number of control parameters that are straightforward to select, automatic adjustment of the control law to accommodate changes to the aerodynamic properties of the vehicle, a complete proof of stability, and facilitated analysis of the effects of model errors. The main motivations for this work were to produce a simplified control design that is also more robust to model error; to accommodate online large changes in the vehicle dynamics, for example, damage, and to learn the aerodynamic coefficient functions for the vehicle. An anticipated benefit from these properties is that the controller could be applied to an aircraft that it was not explicitly designed for, for example, an aircraft of the same family but different configuration. Additionally, the controller could be developed using a lower fidelity model than required by current methods, thereby, offering a cost savings. This control method is expected to provide significant reduction in design time because the control system design does not depend on a conglomeration of point designs. In Ref. 29 some of these benefits are discussed in the context of adaptive control for guided munitions.

The approach herein develops online approximations to the aircraft force and moment functions. Such offline approximations have a long history in the aerodynamics community. Trankle et al. review offline system identification methods in Ref. 30. The example of this paper will use splines in the system identification process. An overview, with several examples, of offline, spline-based, system identification based on data partitioning is presented in Ref. 31. An excellent review of offline estimation of aircraft model parameters from flight data is contained in Ref. 32. Finally, in Ref. 33, offline estimation is performed of additive functional corrections to the aircraft model. The corrections are multidimensional cubic splines (Ref. 33, p. 1294), which is interesting relative to the approach herein where such model error is approximated online.

II. Inner-Loop Control

This section presents an online approximation-based approach to achieve asymptotic perfect tracking (Ref. 22, p. 194) in the aircraft inner loop. The inner-loop controller is presented only for the pitch rate Q. The approach extends directly to control of roll and yaw rates, that is, P and R. We assume that the aerodynamic moments are not known a priori. The controller approximates the moment functions online and uses the approximated moment functions in a feedback-linearizing controller. The control loop is formulated as a tracking problem where the goal is to force Q to converge to and track an arbitrary input signal Q_c, which is differentiable and known. Implicitly, we assume that Q_c is reachable within the actuator constraints, that is, no saturation. Because the derivation and proof are spread through this section, the approach is summarized in equations, Theorem 1, and block diagram (see Fig. 1) in Sec. II.F. Design and analysis of an online approximation-based backstepping controller for γ, α, Q, and V_t is presented in Sec. III by building on the ideas and approach that is presented in the present section.

A. Pitch Rate Model: Q

The Q dynamics are[34]

$$\dot{Q} = f_Q + c_7 \bar{M}(\boldsymbol{x}, \boldsymbol{u}) \tag{1}$$

where $f_Q = c_5 PR - c_6(P^2 - R^2)$ is a known function. The inertial parameters c_5, c_6, and c_7 (defined on p. 80 in Ref. 34) are assumed to be known. The moment $\bar{M}(\boldsymbol{x}, \boldsymbol{u})$ is unknown and is represented here as a function of the entire state x and control vector $\boldsymbol{u}$; however, the online approximation system will only account for the dominant state and control variables, which will be denoted by $\boldsymbol{x}_r$.

For the online approximation-based control design, we manipulate the model into the sum of three functions: known functions,

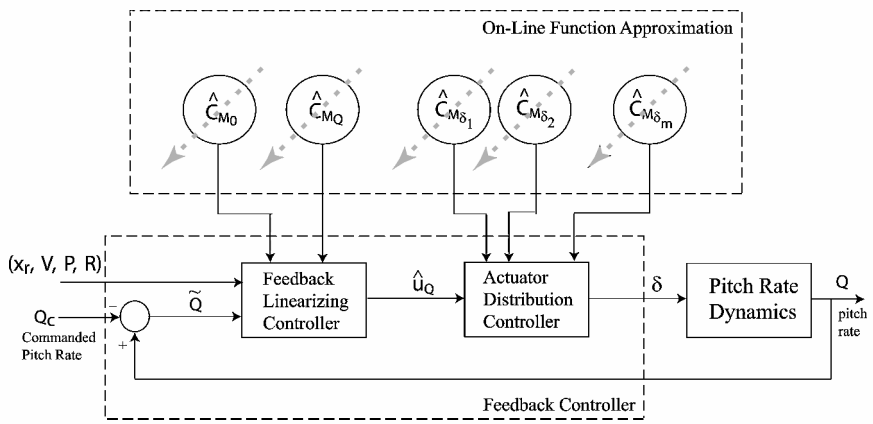

Fig. 1 Block diagram implementation of online approximation-based pitch rate controller.

unknown functions that will be approximated, and residual model errors:

$$\dot{Q} = f_Q + c_7\{\bar{M}(\boldsymbol{x}_r) + [\bar{M}(\boldsymbol{x},\boldsymbol{u}) - \bar{M}(\boldsymbol{x}_r)]\}$$

$$= f_Q + c_7\bar{M}(\boldsymbol{x}_r) + c_7\epsilon_{M_1}(\boldsymbol{x},\boldsymbol{u}) \tag{2}$$

In this representation, we are assuming that the dominant nonlinearities, represented by $\bar{M}(\boldsymbol{x}_r)$, are functions only of a subset of the vehicle state and control variable information denoted by x_r. We assume that the function $\bar{M}(\boldsymbol{x}_r)$ is unknown; therefore, it will be approximated in the control law. The term $\epsilon_{M_1}(\boldsymbol{x},\boldsymbol{u}) = [\bar{M}(\boldsymbol{x},\boldsymbol{u}) - \bar{M}(\boldsymbol{x}_r)]$ is the error between the actual moment and the design model. The error $\epsilon_{M_1}(\boldsymbol{x},\boldsymbol{u})$ is assured to be small due to the assumption that $\bar{M}(\boldsymbol{x}_r)$ is dominant. If this assumption turns out to be incorrect, then additional input variables must be added to $\bar{M}(\boldsymbol{x}_r)$ to validate the assumption that this term is dominant.

Using coefficient notation similar to that which is typical for aircraft, we represent the pitch moment design model as

$$\bar{M}(\boldsymbol{x}_r) = \bar{q}S\bar{c}\left[C_{M_o}(\boldsymbol{x}_r) + C_{M_Q}(\boldsymbol{x}_r)\frac{\bar{c}Q}{2V} + \sum_{i=1}^{m} C_{M_{\delta_i}}(\boldsymbol{x}_r)\delta_i\right] \tag{3}$$

$$\bar{M}(\boldsymbol{x}_r) = \bar{q}S\bar{c}\left[C_{M_o}(\boldsymbol{x}_r) + C_{M_Q}(\boldsymbol{x}_r)\frac{\bar{c}Q}{2V}\right] + u_Q \tag{4}$$

where the scalar control moment is $u_Q = G_Q\boldsymbol{\delta}$ and $G_Q = \bar{q}S\bar{c}[C_{M_{\delta_1}}(\boldsymbol{x}_r), \ldots, C_{M_{\delta m}}(\boldsymbol{x}_r)]$. Note that the error $\epsilon_{M_1}(\boldsymbol{x},\boldsymbol{u})$ can be reduced by adding additional coefficient terms, for example, $C_{M_o}(\boldsymbol{x}_r)$ to Eqs. (3) and (4). The vector $\boldsymbol{\delta}$ represents the vector of (total) control surface deflections, not a perturbation relative to a set point.

The control design approach is to specify u_Q to attain tracking of Q_c by Q, then to perform actuator distribution to specify the actuator signals of the vector $\boldsymbol{\delta}$. Actuator distribution, which is an interesting problem itself will not be discussed here. Several actuator distribution approaches are available.[35–38]

B. Control Approach for a Known Model

If the function $\bar{M}(\boldsymbol{x}_r)$ were known, then the designer could select the feedback-linearizing control law

$$u_Q = -(\bar{q}S\bar{c})\left[C_{M_o}(\boldsymbol{x}_r) + C_{M_Q}(\boldsymbol{x}_r)(\bar{c}Q/2V)\right]$$

$$+ (1/c_7)\left(-f_Q - K_Q\tilde{Q} - K_{Q_I}\tilde{Q}_I + \dot{Q}_c + \eta_Q\right) \tag{5}$$

where

$$\tilde{Q} = (Q - Q_c), \qquad \tilde{Q}_I = \int \tilde{Q}\,\mathrm{d}t$$

The signal η_Q is added (if desired) to dominate the effect of model errors. It is inserted here for completeness and will be discussed later. The control law defined earlier would yield the tracking error dynamics:

$$\dddot{\tilde{Q}}_I + K_Q\ddot{\tilde{Q}}_I + K_{Q_I}\dot{\tilde{Q}}_I = c_7\epsilon_{M_1}(\boldsymbol{x},\boldsymbol{u}) + \eta_Q \tag{6}$$

These error dynamics show that the transient response of the Q loop to disturbances or initial condition errors is determined by the roots of $s^2 + K_Q s + K_{Q_I} = 0$. Therefore, K_Q and K_{Q_I} are positive parameters selected to design this transient response. The tracking error dynamics are excited by the modeling error $\epsilon_{M_1}(\boldsymbol{x},\boldsymbol{u})$.

C. Control Approach for an Unknown Model

The function $\bar{M}(\boldsymbol{x}_r)$ may be inaccurate or may change during flight; therefore, it will be approximated online. The approximation will be denoted $\hat{M}(\boldsymbol{x}_r)$, where $\hat{M}(\boldsymbol{x}_r)$ has the same structure as $\bar{M}(\boldsymbol{x}_r)$:

$$\hat{M}(\boldsymbol{x}_r) = \bar{q}S\bar{c}\left[\hat{C}_{M_o}(\boldsymbol{x}_r) + \hat{C}_{M_Q}(\boldsymbol{x}_r)\frac{\bar{c}Q}{2V} + \sum_{i=1}^{m}\hat{C}_{M_{\delta_i}}(\boldsymbol{x}_r)\boldsymbol{\delta}_i\right]$$

where $\hat{u}_Q = \bar{q}S\bar{c}[\hat{C}_{M_{\delta_i}}, \ldots, \hat{C}_{M_{\delta m}}] = \bar{q}S\bar{c}\hat{G}_Q$ and the aerodynamic coefficient functions $\hat{C}_{M_o}(\boldsymbol{x}_r)$, $\hat{C}_{M_Q}(\boldsymbol{x}_r)$, and $\hat{C}_{M_{\delta_i}}(\boldsymbol{x}_r)$ are not known and will be approximated by the control law. Note that any prior available information about $\bar{M}(\boldsymbol{x}_r)$ can be used to initialize $\hat{M}(\boldsymbol{x}_r)$, but this is not required.

When $\hat{M}(\boldsymbol{x}_r)$ is used in the control law, the control law is

$$\hat{u}_Q = -(\bar{q}S\bar{c})\left[\hat{C}_{M_o}(\boldsymbol{x}_r) + \hat{C}_{M_Q}(\boldsymbol{x}_r)(\bar{c}Q/2V)\right]$$

$$+ (1/c_7)\left(-f_Q - K_Q\tilde{Q} - K_{Q_I}\tilde{Q}_I + \dot{Q}_c + \eta_Q\right)$$

with the total surface deflections $\boldsymbol{\delta}$ selected such that $\hat{u}_Q = \hat{G}_Q(\boldsymbol{x}_r)\boldsymbol{\delta}$ by one of the available actuator distribution methods. For actuator distribution to succeed, the estimated actuator distribution matrix $\hat{G}_Q$ must have full row rank. Note that it is possible for $\hat{G}_Q$ to lose row rank even when G_Q does not. This is an issue related to the transient of the parameter estimation process. It can by avoided either by projection methods[39] or by adding excitation to $\boldsymbol{\delta}$ that lies in the null space of $\hat{G}_Q$ when the $\det(\hat{G}_Q\hat{G}_Q^T)$ becomes too close to zero.

When started from Eq. (2), the Q tracking error dynamics simplify as follows:

$$\dot{Q} = f_Q + c_7\hat{M} + c_7\left[\bar{M} - \hat{M} + \epsilon_{M_1}(\boldsymbol{x},\boldsymbol{u})\right]$$

$$= f_Q + c_7\bar{q}S\bar{c}\left[\hat{C}_{M_o} + \hat{C}_{M_Q}(\bar{c}Q/2V)\right] + c_7\hat{u}_Q$$

$$+ c_7\left[\bar{M} - \hat{M} + \epsilon_{M_1}(\boldsymbol{x},\boldsymbol{u})\right]$$

$$\dddot{\tilde{Q}}_I + K_Q\ddot{\tilde{Q}}_I + K_{Q_I}\dot{\tilde{Q}}_I = c_7\left[\bar{M} - \hat{M} + \epsilon_{M_1}(\boldsymbol{x},\boldsymbol{u})\right] + \eta_Q \tag{7}$$

Note that at this point in the analysis, online approximation has not yet been introduced. Therefore, Eq. (7) applies also to fixed-gain control and shows that the tracking error is driven by error between the actual moment $\bar{M} + \epsilon_{M_1}$ and the design model $\bar{M}$. Online approximation will be used to decrease this model error or any additional model error that arises from online events, for example, battle damage.

D. Online Approximator Structure

The coefficient functions to be approximated will be represented by linear-in-the-parameter approximations

$$\hat{C}_{M_o}(\boldsymbol{x}_r) = \theta_{M_o}^T\phi_{M_o}(\boldsymbol{x}_r) \tag{8}$$

$$\hat{C}_{M_Q}(\boldsymbol{x}_r) = \theta_{M_Q}^T\phi_{M_Q}(\boldsymbol{x}_r) \tag{9}$$

$$\hat{C}_{M_{\delta_i}}(\boldsymbol{x}_r) = \theta_{M_{\delta_i}}^T\phi_{M_{\delta_i}}(\boldsymbol{x}_r), \qquad i = 1, \ldots, m \tag{10}$$

where $\boldsymbol{x}_r \in \Re^d$. Although this representation allows different basis functions for each coefficient function, for simplicity of notation we will assume that $\phi_{M_o}(\boldsymbol{x}_r) = \phi_{M_Q}(\boldsymbol{x}_r) = \phi_{M_{\delta_i}}(\boldsymbol{x}_r) = \phi(\boldsymbol{x}_r)$, where $\phi(\boldsymbol{x}_r)$: $\Re^d \mapsto \Re^N$ is a regressor vector containing the basis functions for the approximation. Finally, $\Theta_M = [\theta_{M_o}, \theta_{M_Q}, \theta_{M_{\delta_1}}, \ldots, \theta_{M_{\delta m}}] \in \Re^{N\times(2+m)}$ is the matrix of parameters for the $(2+m)$ approximated functions.

Denote the operating envelope by $\mathcal{D}$, which is assumed to be compact, that is, closed and bounded. Then for continuous $\bar{M}(\boldsymbol{x}_r)$, there exists optimal moment approximation parameters Θ_M^* such that

$$\Theta_M^* = \mathrm{argmin}_{\Theta_M}\left[\sup_{\mathcal{D}}\left|\bar{M}(\boldsymbol{x}_r) - \bar{q}S\bar{c}\left(\theta_{M_o}^T + \theta_{M_Q}^T\frac{\bar{c}Q}{2V}\right.\right.\right.$$

$$\left.\left.\left. + \sum_{i=1}^{m}\theta_{M_{\delta_i}}^T\delta_i\right)\phi(\boldsymbol{x}_r)\right|\right]$$

$$\bar{\epsilon}_{M_2} = \sup_{\mathcal{D}}|\epsilon_{M_2}(\boldsymbol{x}_r)| < \infty$$

where

$$\epsilon_{M_2}(\boldsymbol{x}_r) = \left[\bar{M}(\boldsymbol{x}_r) - \bar{q} S \bar{c} \left(\theta_{M_o}^T + \theta_{M_Q}^T \frac{\bar{c} Q}{2V} + \sum_{i=1}^{m} \theta_{M_{\delta_i}}^T \delta_i \right) \Bigg|_{\Theta_M = \Theta_M^*} \phi(\boldsymbol{x}_r) \right]$$

Because the designer has the freedom to choose the basis set $\phi(\,)$, it can be selected so that $\bar{\epsilon}_{M_2}$ is small. Note that the values of Θ_M^* and $\bar{\epsilon}_{M_2}$ need not be known. These quantities are not used in the control calculations. It is sufficient to know that these quantities exist.

Two model error terms have been introduced. The term ϵ_{M_1} is the error incurred by neglecting some of the state variables in the model representation of the moment. This error could be reduced by including additional input variables in the moment model or by including additional aerodynamic coefficients, at the expense of requiring additional memory and computation. The term ϵ_{M_2} is the approximation error incurred due to the choice of the approximator basis set. This error can be reduced by increasing the number of basis elements. There is an inherent tradeoff. Reduction of either error will require additional computation. Therefore, both the regression vector and the dimension of the input space must be selected judiciously.

With the preceding definition of Θ_M^* and $\bar{\epsilon}_{M_2}$, we can write

$$\bar{M}(\boldsymbol{x}_r) = \bar{q} S \bar{c} \left(\theta_{M_o}^T + \theta_{M_Q}^T \frac{\bar{c} Q}{2V} + \sum_{i=1}^{m} \theta_{M_{\delta_i}}^T \delta_i \right) \Bigg|_{\Theta_M^*} \phi(\boldsymbol{x}_r) + \epsilon_{M_2}(\boldsymbol{x}_r)$$

Define the parameter error vectors as $\tilde{\theta}_{M_o} = \theta_{M_o} - \theta_{M_o}^*$, $\tilde{\theta}_{M_Q} = \theta_{M_Q} - \theta_{M_Q}^*$, $\tilde{\theta}_{M_{\delta_i}} = \theta_{M_{\delta_i}} - \theta_{M_{\delta_i}}^*$, and $\tilde{\Theta}_M = \Theta_M - \Theta_M^*$. Then, the tracking error dynamics from Eq. (7) can be further manipulated as

$$\ddot{\tilde{Q}}_I + K_Q \dot{\tilde{Q}}_I + K_{Q_I} \tilde{Q}_I = -c_7 \bar{q} S \bar{c} \left[\left(\tilde{\theta}_{M_o}^T + \tilde{\theta}_{M_Q}^T \frac{\bar{c} Q}{2V} + \sum_{i=1}^{m} \tilde{\theta}_{M_{\delta_i}}^T \delta_i \right) \phi(\boldsymbol{x}_r) \right] + c_7 \left[\epsilon_{M_2}(\boldsymbol{x}_r) + \epsilon_{M_1}(\boldsymbol{x}, \boldsymbol{u}) \right] + \eta_Q \quad (11)$$

Therefore, the transient response to disturbances and initial condition errors is still determined by the roots of $s^2 + K_Q s + K_{Q_I} = 0$. The tracking error is excited by the errors in the parameters of the approximated functions $\tilde{\Theta}_M = [\tilde{\theta}_{M_o}, \tilde{\theta}_{M_Q}, \tilde{\theta}_{M_{\delta_1}}, \ldots, \tilde{\theta}_{M_{\delta m}}]$ and by the residual approximation errors $(\epsilon_{M_2} + \epsilon_{M_1})$. The next step is to derive parameter adaptation laws for the approximation parameter vectors, so that $\tilde{Q}$ and $\tilde{\Theta}_M$ have desirable stability properties.

E. Stability and Parameter Adaptation

When the pitch rate tracking error state vector is defined as $\boldsymbol{z} = [\tilde{Q}_I, \dot{\tilde{Q}}]^T$, Eq. (11) can be written in state-space form as

$$\dot{\boldsymbol{z}} = A\boldsymbol{z} + B u$$

where

$$u = -c_7 \bar{q} S \bar{c} \left[\left(\tilde{\theta}_{M_o}^T + \tilde{\theta}_{M_Q}^T \frac{\bar{c} Q}{2V} + \sum_{i=1}^{m} \tilde{\theta}_{M_{\delta_i}}^T \delta_i \right) \phi(\boldsymbol{x}_r) \right] + c_7 \left[\epsilon_{M_2}(\boldsymbol{x}_r) + \epsilon_{M_1}(\boldsymbol{x}, \boldsymbol{u}) \right] + \eta_Q$$

$$B = \begin{bmatrix} 0 \\ 1 \end{bmatrix}, \qquad A = \begin{bmatrix} 0 & 1 \\ -K_{Q_I} & -K_Q \end{bmatrix}$$

Define the Lyapunov function

$$\mathcal{V} = \boldsymbol{z}^T P_z \boldsymbol{z} + \frac{1}{2} \left(\tilde{\theta}_{M_o}^T \Gamma_{M_o}^{-1} \tilde{\theta}_{M_o} + \tilde{\theta}_{M_Q}^T \Gamma_{M_Q}^{-1} \tilde{\theta}_{M_Q} + \sum_{i=1}^{m} \tilde{\theta}_{M_{\delta_i}}^T \Gamma_{M_{\delta_i}}^{-1} \tilde{\theta}_{M_{\delta_i}} \right) \quad (12)$$

where Γ_{M_o}, Γ_{M_Q}, and $\Gamma_{M_{\delta_i}}$, $i = 1, \ldots, m$, are symmetric, positive definite, and dimensionless parameter adaptation gain matrices and $P_z = P_z^T > 0$ is the solution to $A^T P_z + P_z A = -I$. Define $e = (P_z B)^T \boldsymbol{z} = \boldsymbol{z}^T P_z B$, where

$$P_z B = \begin{bmatrix} \dfrac{1}{2K_{Q_I}} \\ \dfrac{1}{2} \dfrac{1 + K_{Q_I}}{K_{Q_I} K_Q} \end{bmatrix}$$

The time derivative of $\mathcal{V}$ along solutions of the closed-loop Q online approximation-based control system is

$$\begin{aligned} \dot{\mathcal{V}} &= -\boldsymbol{z}^T \boldsymbol{z} - \boldsymbol{z}^T P_z B c_7 (\bar{q} S \bar{c}) \\ &\quad \times \left[\left(\tilde{\theta}_{M_o}^T + \tilde{\theta}_{M_Q}^T \frac{\bar{c} Q}{2V} + \sum_{i=1}^{m} \tilde{\theta}_{M_{\delta_i}}^T \delta_i \right) \phi(\boldsymbol{x}_r) \right] \\ &\quad + \boldsymbol{z}^T P_z B c_7 \left[\epsilon_{M_2}(\boldsymbol{x}_r) + \epsilon_{M_1}(\boldsymbol{x}, \boldsymbol{u}) \right] + \boldsymbol{z}^T P_z B \eta_Q \\ &\quad + \left[\tilde{\theta}_{M_o}^T \Gamma_{M_o}^{-1} \dot{\theta}_M + \tilde{\theta}_{M_Q}^T \Gamma_{M_Q}^{-1} \dot{\theta}_{M_Q} + \sum_{i=1}^{m} \tilde{\theta}_{M_{\delta_i}}^T \Gamma_{M_{\delta_i}}^{-1} \dot{\theta}_{M_{\delta_i}} \right] \\ &= -\boldsymbol{z}^T \boldsymbol{z} - e c_7 (\bar{q} S \bar{c}) \left[\left(\tilde{\theta}_{M_o}^T + \tilde{\theta}_{M_Q}^T \frac{\bar{c} Q}{2V} + \sum_{i=1}^{m} \tilde{\theta}_{M_{\delta_i}}^T \delta_i \right) \phi(\boldsymbol{x}_r) \right] \\ &\quad + e c_7 \left[\epsilon_{M_2}(\boldsymbol{x}_r) + \epsilon_{M_1}(\boldsymbol{x}, \boldsymbol{u}) \right] + \eta_Q e \\ &\quad + \left[\tilde{\theta}_{M_o}^T \Gamma_{M_o}^{-1} \dot{\theta}_M + \tilde{\theta}_{M_Q}^T \Gamma_{M_Q}^{-1} \dot{\theta}_{M_Q} + \sum_{i=1}^{m} \tilde{\theta}_{M_{\delta_i}}^T \Gamma_{M_{\delta_i}}^{-1} \dot{\theta}_{M_{\delta_i}} \right] \end{aligned}$$

Then, when the adaptation laws are chosen as

$$\dot{\theta}_{M_o} = c_7 (\bar{q} S \bar{c}) e \Gamma_{M_o} \phi(\boldsymbol{x}_r) \quad (13)$$

$$\dot{\theta}_{M_Q} = c_7 (\bar{q} S \bar{c}) e \Gamma_{M_Q} \phi(\boldsymbol{x}_r) (\bar{c} Q / 2V) \quad (14)$$

$$\dot{\theta}_{M_{\delta i}} = c_7 (\bar{q} S \bar{c}) e \Gamma_{M_{\delta_i}} \phi(\boldsymbol{x}_r) \boldsymbol{\delta}_i, \qquad i = 1, \ldots, m, \quad (15)$$

the time derivative of $\mathcal{V}$ reduces to

$$\begin{aligned} \dot{\mathcal{V}} &= -\boldsymbol{z}^T \boldsymbol{z} + e c_7 \left[\epsilon_{M_2}(\boldsymbol{x}_r) + \epsilon_{M_1}(\boldsymbol{x}, \boldsymbol{u}) \right] + \eta_Q e \\ &\leq -\|\boldsymbol{z}\|^2 + \|\boldsymbol{z}\| \|P_z B\| c_7 \bar{\epsilon} + \eta_Q e \end{aligned} \quad (16)$$

where $\bar{\epsilon}$ is an upper bound on the modeling error, for example, $\bar{\epsilon} = \sup_{\mathcal{D}} |\epsilon_{M_2}(\boldsymbol{x}_r) + \epsilon_{M_1}(\boldsymbol{x}, \boldsymbol{u})|$.

In the case where $\eta_Q = 0$, Eq. (16) is of the same form as Eq. (A3) of Appendix A. (Note that the term $c_7 \bar{q} S \bar{c}$ is always positive.) Therefore, the proof proceeds similarly to show that $\boldsymbol{z}$ and $\tilde{\Theta}_M \in \mathcal{L}_\infty$ and that $\|\boldsymbol{z}\|$ is $\bar{\epsilon}^2$ small in the mean-squared sense (MSS), that is, $\|\boldsymbol{z}\| \in S(\bar{\epsilon}^2)$. Additionally, $\|\boldsymbol{z}\|$ is asymptotically uniformly bounded by

$$\|\boldsymbol{z}\| \leq \frac{\bar{\lambda}(P_z)}{\underline{\lambda}(P_z)} \|P_z B\| c_7 \bar{\epsilon} = c_7 \bar{\epsilon} \frac{\bar{\lambda}(P_z)}{\underline{\lambda}(P_z)} \frac{\sqrt{K_Q^2 + \left(K_{Q_I} + 1\right)^2}}{2 K_Q K_{Q_I}}$$

where $\bar{\lambda}(P_z)$ and $\underline{\lambda}(P_z)$ are the maximum and minimum eigenvalues of P_z. Alternatively, if $\eta_Q = K g(e)$, where $e g(e) < 0$ and $K |g(e)| > c_7 |\epsilon_{M_2}(\boldsymbol{x}_r) + \epsilon_{M_1}(\boldsymbol{x}, \boldsymbol{u})|$, then the system is asymptotically stable. If $\eta_Q = K g(e)$ with $K > 0$ where $e g(e) < 0$, but $K |g(e)|$ is not always greater than $c_7 |\epsilon_{M_2}(\boldsymbol{x}_r) + \epsilon_{M_1}(\boldsymbol{x}, \boldsymbol{u})|$, then $\boldsymbol{z}$ and $\tilde{\Theta}_M \in \mathcal{L}_\infty$; $\|\boldsymbol{z}\|$ is $\bar{\epsilon}^2$ small in the MSS, that is, $\|\boldsymbol{z}\| \in S(\bar{\epsilon}^2)$, and $\|\boldsymbol{z}\|$ is asymptotically uniformly bounded with a bound at least as small

as that defined earlier. In all of the cases described in this paragraph, the asymptotic uniform bound is proportional to $\bar{\epsilon}$, which is small.

This approach can be reformulated and the proofs will go through for the case where $K_{Q_I} = 0$. In this section we have included the nonzero K_{Q_I} term because it ensures that the integral of the Q error, that is, pitch error, remains small during function approximation transients. The reformulation with $K_{Q_I} = 0$ is not included herein, but is straightforward. The control law depends on $[\bar{c}, S, c_5, c_6, c_7]$. Therefore, error in these values will affect the size of the residual modeling error and, hence, the performance of the feedback linearizing controller. Each of these parameters is typically known relatively accurately.

When $\|z\| < \|P_z B\| c_7 \bar{\epsilon}$, a deadzone should be included in the adaptive law to prevent parameter updates. Without such a deadzone, stability is not guaranteed, and the parameters could drift. Implementation of the deadzone requires knowledge of $\bar{\epsilon}$ or an upper bound on it. As currently defined, the size of the deadzone $\bar{\epsilon}$ is a constant upper bound on the modeling error for the whole region $\mathcal{D}$. If the region is relatively large, then a fixed bound on $\bar{\epsilon}$ can be conservative, which would create a large deadzone. One approach to remedy this issue is to have a time-varying deadzone, which is a function of the measured state, for example, Q. This is especially important in online approximation schemes because by nature we are trying to expand the operating region $\mathcal{D}$. Because such issues are not our main focus, they are not discussed herein. The design of such a time-varying deadzone is described in Refs. 27 and 40. Leakage or σ modifications are two alternative methods for achieving robustness of the online approximation to noise, disturbances, and residual approximation error.[39] Implementation could be achieved by augmentation of Eqs. (13–15) with additional additive terms. If the parameters are known to lie in a convex set $\mathcal{S}$, then projection methods can be used to ensure that the parameter estimates do not leave $\mathcal{S}$. For example, projection methods can be used to ensure the sign of the control coefficients $\hat{C}_{M_{\delta_i}}$ is maintained. If projection is used, then the stability proofs still go through using arguments similar to those given in Ref. 39.

F. Inner-Loop Control Summary

The equations of the online approximation based controller follow.

For the inner-loop control law

$$\hat{u}_Q = -\bar{q} S \bar{c} \left[\hat{C}_{M_o}(\boldsymbol{x}_r) + \hat{C}_{M_Q}(\boldsymbol{x}_r)(\bar{c} Q / 2V) \right] + (1/c_7)\left(-f_Q - K_Q \tilde{Q} - K_{Q_I} \tilde{Q}_I + \dot{Q}_c + \eta_Q \right)$$

Select $\boldsymbol{\delta}$ such that $\hat{u}_Q = \hat{G}_Q \boldsymbol{\delta}$.

$$\hat{G}_Q = \bar{q} S \bar{c} \left[\hat{C}_{M_{\delta_1}}(\boldsymbol{x}_r), \ldots, \hat{C}_{M_{\delta m}}(\boldsymbol{x}_r) \right]$$

The approximated moment coefficients are

$$\hat{C}_{M_o}(\boldsymbol{x}_r) = \theta_{M_o}^T \phi(\boldsymbol{x}_r), \qquad \hat{C}_{M_Q}(\boldsymbol{x}_r) = \theta_{M_Q}^T \phi(\boldsymbol{x}_r)$$

$$\hat{C}_{M_{\delta_i}}(\boldsymbol{x}_r) = \theta_{M_{\delta_i}}^T \phi(\boldsymbol{x}_r), \qquad i = 1, \ldots, m$$

The parameter adaptation equations are specified in Eqs. (13–15) $\tilde{Q}_I$ is the integrated pitch rate error. K_Q and K_{Q_I} are control gains, $\phi(\boldsymbol{x}_r)$ is a basis for the function approximation, and the remaining variables and parameters are defined in the Nomenclature.

The properties of this controller are summarized in Theorem 1 for an aircraft with m control surfaces. A block diagram implementation of the controller is shown in Fig. 1.

Theorem 1: The control law summarized in the preceeding equations stabilizes the Q dynamics of an aircraft in the sense that 1) $|\tilde{Q}|$ is ultimately bounded by

$$c_7 \bar{\epsilon} \frac{\bar{\lambda}(P_z)}{\underline{\lambda}(P_z)} \frac{\sqrt{K_Q^2 + \left(K_{Q_I} + 1\right)^2}}{2 K_Q K_{Q_I}}$$

(Ref. 20, definition 4.4), 2) $\tilde{Q} \in \mathcal{L}_\infty$, 3) $\Theta_M \in \mathcal{L}_\infty$, and 4) $\tilde{Q}$ is $\bar{\epsilon}^2$ small in the MSS, where K_Q and K_{Q_I} are positive control gains, $\bar{\epsilon}$ is a bound on $|\epsilon_{M_1} + \epsilon_{M_2}|$, $\Theta_M = [\theta_{M_o}, \theta_{M_Q}, \theta_{M_{\delta_1}}, \ldots, \theta_{\delta m}]$, and the remaining variable and parameters are defined in the Nomenclature. The term $\bar{\epsilon}^2$ small in the MSS is defined in Appendix A.

Note that the modeling error terms ϵ_{M_1} and ϵ_{M_2} can be made arbitrarily small by appropriate selection of the model structure in Eq. (3) and the selection of the basis set $\phi(\boldsymbol{x}_r)$ already given. The parameters K_Q and K_{Q_I} should be selected to specify the tracking error dynamics. The desired tracking error dynamics should be defined to achieve the specified handling qualities. The control law assumes that both Q_c and $\dot{Q}_c$ are available, bounded, and specify the desired trajectory to be tracked. The boundedness and derivative availability requirements can be enforced by passing a arbitrary bounded trajectory Q_r through a strictly proper low pass prefilter of at least first order.

Note that the convergence of $\tilde{\Theta}_M$ to zero is not required for the tracking error to have the properties stated in Theorem 1. Theorem 1 only states that the approximator parameters are bounded; in fact, they tend to converge toward the optimal set of parameters required to approximate the moment function. If the regressor vector satisfies certain excitation conditions, then this parameter convergence is exponential to a region with size determined by ϵ_{M_1} and ϵ_{M_2}. The trajectory of the approximator parameters is such that the function approximation error is locally decreased in the vicinity of the current operating point. If the basis elements have local support, then the approximated functions are not changed in regions distant from the present operating point.[25] If the basis elements do not have local support, then the approximation error in distant regions of the operating envelope might increase when the parameters are tuned to decrease the model error at the present operating point; however, the Lyapunov function $\mathcal{V}$ is nonincreasing.

III. Outer-Loop Control

This section presents an online approximation-based approach to achieve asymptotic perfect tracking for the flight-path angle γ and the airspeed V. To control γ using backstepping, the designer can choose either angle of attack α or pitch $\theta = \alpha + \gamma$ as an intermediate variable. Subsection III.C presents a backstepping-based approach for the control of γ, α, Q, and V. In this approach, the controller will force α and Q to track the internally generated command signals α_c and Q_c. A backstepping controller using θ as the intermediate variable can be similarly derived.[41,42]

An online approximation-based version of the γ, α, Q, and V backstepping controller is presented in Sec. III.D. In this approach, we do not assume that the aerodynamic drag and lift force and pitch moment are known a priori. The controller approximates the drag and lift force and pitch moment functions online and uses the approximated functions in a backstepping controller. Perfect tracking is achieved asymptotically as the approximated functions converge. The implementation equations are summarized in Sec. III.E. The theoretical properties of the controller are summarized in Theorem 2.

A. Longitudinal Model: γ, α, Q, and V

The flight-path angle is defined as (Ref. 34, pp. 88 and 131)

$$\gamma = \sin^{-1}(\dot{h}/V) \tag{17}$$

where h is the aircraft altitude. If the aircraft dynamics are restricted to the pitch plane, then $\gamma = \theta - \alpha$. Then the γ dynamics are

$$\dot{\gamma} = \frac{L}{mV} + \left[\frac{T \sin(\alpha) - mg \cos(\gamma)}{mV} \right] = \frac{L}{mV} + f_\gamma(\alpha, T, V, \gamma)$$

where

$$f_\gamma = \left[\frac{T \sin(\alpha) - mg \cos(\gamma)}{mV} \right]$$

is a known function. Therefore, we have the following four dynamic equations:

$$\dot{\gamma} = (L/mV) + f_\gamma, \qquad \dot{\alpha} = -(L/mV) + Q - f_\gamma$$

$$\dot{Q} = c_7\bar{M} + f_Q, \qquad \dot{V} = (1/m)[T\cos(\alpha) - D - mg\sin(\theta - \alpha)]$$

B. Lift and Drag Representation

We will work with the standard aircraft coefficient notation. Therefore, the structure of the actual lift and drag functions are assumed to be of the form

$$L(\boldsymbol{x}, \boldsymbol{\delta}) = \bar{q}S\left[C_L(\boldsymbol{x}_r) + C_{L_\alpha}(\boldsymbol{x}_r)\alpha\right] + \epsilon_{L_1}(\boldsymbol{x}, \boldsymbol{\delta})$$

$$D(\boldsymbol{x}, \boldsymbol{\delta}) = \bar{q}S\left[C_D(\boldsymbol{x}_r) + \sum_{i=1}^{m} C_{D_{\delta_i}}(\boldsymbol{x}_r)|\boldsymbol{\delta}_i|\right] + \epsilon_{D_1}(\boldsymbol{x}, \boldsymbol{\delta})$$

The two lift coefficients $C_L(\boldsymbol{x}_r)$ and $C_{L_\alpha}(\boldsymbol{x}_r)$ and the $(m+1)$ drag coefficients are sufficient to illustrate the method. The main assumption is that $\epsilon_{L_1}(\boldsymbol{x}, \boldsymbol{\delta})$ and $\epsilon_{D_1}(\boldsymbol{x}, \boldsymbol{\delta})$ are small for $\boldsymbol{x}$ in the operating envelope $\mathcal{D}$. Additional coefficients may be required depending on the characteristics of the aircraft to be controlled. The vector variable $\boldsymbol{x}_r$ represents the subset of the vehicle state and control vector information that dominates the functional dependence of the lift and drag functions. This is clarified further in the example of Sec. IV. The pitch moment is modeled as described in Sec. II.A.

Using the aerodynamic coefficient notation, the γ, α, Q, and V dynamic equations are

$$\dot{\gamma} = \frac{\bar{q}S\left(C_L + C_{L_\alpha}\alpha\right)}{mV} + f_\gamma + \frac{\epsilon_{L_1}}{mV}$$

$$\dot{\alpha} = -\frac{\bar{q}S\left(C_L + C_{L_\alpha}\alpha\right)}{mV} + Q - f_\gamma - \frac{\epsilon_{L_1}}{mV}$$

$$\dot{Q} = f_Q + c_7\left[\bar{q}S\bar{c}\left(C_{M_o} + C_{M_Q}\frac{\bar{c}Q}{2V}\right) + u_Q + \epsilon_{M_1}\right]$$

$$\dot{V} = \frac{1}{m}\left[T\cos(\alpha) - \bar{q}S\left(C_D + \sum_{i=1}^{m} C_{D_{\delta_i}}|\delta_i|\right) - mg\sin(\theta - \alpha) - \epsilon_{D_1}\right]$$

where $(\boldsymbol{x}_r)$ has been dropped to reduce the complexity of the notation. Assume that the externally generated signals $(\gamma_c, \dot{\gamma}_c)$ and $(V_c, \dot{V}_c)$ are bounded and available. Then, the dynamic equations for the tracking errors $\tilde{\gamma} = \gamma - \gamma_c$, $\tilde{\alpha} = \alpha - \alpha_c$, $\tilde{Q} = Q - Q_c$, and $\tilde{V} = V - V_c$ are

$$\dot{\tilde{\gamma}} = \frac{\bar{q}S\left[C_L + C_{L_\alpha}(\alpha_c + \tilde{\alpha})\right]}{mV} + f_\gamma - \dot{\gamma}_c + \frac{\epsilon_{L_1}}{mV} \tag{18}$$

$$\dot{\tilde{\alpha}} = -\frac{\bar{q}S\left(C_L + C_{L_\alpha}\alpha\right)}{mV} + Q_c + \tilde{Q} - f_\gamma - \dot{\alpha}_c - \frac{\epsilon_{L_1}}{mV} \tag{19}$$

$$\dot{\tilde{Q}} = c_7\bar{q}S\bar{c}\left(C_{M_o} + C_{M_Q}\frac{\bar{c}Q}{2V}\right) + c_7u_Q + f_Q - \dot{Q}_c + c_7\epsilon_{M_1} \tag{20}$$

$$\dot{\tilde{V}} = \frac{1}{m}\left[T\cos(\alpha) - \bar{q}S\left(C_D + \sum_{i=1}^{m} C_{D_{\delta_i}}|\delta_i|\right)\right] - g\sin(\gamma) - \dot{V}_c - \frac{\epsilon_{D_1}}{m} \tag{21}$$

The variables (α_c, Q_c) and their derivatives will be discussed next.

C. Backstepping Control of γ, α, Q, and V: Known Aerodynamic Functions

In the case where the lift and moment functions are known, the backstepping control signals can be selected as follows:

$$\alpha_c = \frac{1}{C_{L_\alpha}}\left[-C_L + \frac{mV}{\bar{q}S}(-f_\gamma + \dot{\gamma}_c - K_\gamma\tilde{\gamma} + \nu_\gamma)\right] \tag{22}$$

$$Q_c = \frac{\bar{q}S\left(C_L + C_{L_\alpha}\alpha\right)}{mV} - K_\alpha\tilde{\alpha} + f_\gamma + \dot{\tilde{\alpha}}_c + \nu_\alpha - \tilde{\gamma}\frac{\bar{q}SC_{L_\alpha}}{mV} \tag{23}$$

$$u_Q = -\bar{q}S\bar{c}\left(C_{M_o} + C_{M_Q}\frac{\bar{c}Q}{2V}\right) + \frac{-K_Q\tilde{Q} + \nu_Q - \tilde{\alpha} + \dot{\tilde{Q}}_c - f_Q}{c_7} \tag{24}$$

$$T = \left\{\bar{q}S\left(C_D + \sum_{i=1}^{m} C_{D_{\delta_i}}|\delta_i|\right) + mg\sin(\gamma) + m[\dot{V}_c - K_v(V - V_c) + \nu_V]\right\} \Big/ \cos(\alpha) \tag{25}$$

where $\dot{\tilde{\alpha}}_c$ is an approximation to $\dot{\alpha}_c$. At least three approaches to handle the term $\dot{\alpha}_c$ are possible: 1) Compute $\dot{\alpha}_c$ exactly. This is complex and requires knowledge of $\dot{\alpha}$, which is not generally available directly. Also, exact computation does not extend conveniently to adaptive or online approximation-based approaches. 2) Neglect $\dot{\alpha}_c$ completely. This would require increasing the upper bound $\bar{\epsilon}$ on the modeling errors enough to overbound the entire command derivative. 3) Use a filtered version of the derivative in place of the derivative, for example, $\dot{\tilde{\alpha}}_c = [s/(\tau_\alpha s + 1)]\alpha_c$. In this case, $\bar{\epsilon}$ only is increased by the error between the derivative and the filtered derivative. The presentation to follow applies to any of these choices, but the authors favor method 3 and use it in the simulation example. Method 3 works well because the signal that is being filtered is continuous. Therefore, the signal energy is at low frequencies where the filter is a good approximation to the derivative. Note that this is by design because the designer selects the bandwidth of the derivative filter, that is, $1/\tau_\alpha$, and the bandwidth of α_c, that is, K_γ. In Eqs. (22–25), $\dot{\tilde{Q}}_c$ is an approximation to $\dot{Q}_c$; for example, $\tilde{Q}_c = [s/(\tau_Q s + 1)]Q_c$ (see the comments for $\dot{\tilde{\alpha}}_c$). K_γ, K_α, K_Q, and K_V are positive control gains and ν_γ, ν_α, ν_Q, and ν_V are terms that will be defined later to ensure robustness to modeling errors. Then, the controlled tracking error dynamics are

$$\dot{\tilde{\gamma}} = -K_\gamma\tilde{\gamma} + \nu_\gamma + \tilde{\alpha}\left(\bar{q}SC_{L_\alpha}/mV\right) + \epsilon_{L_1}/mV \tag{26}$$

$$\dot{\tilde{\alpha}} = -K_\alpha\tilde{\alpha} + \nu_\alpha + \tilde{Q} + (\dot{\tilde{\alpha}}_c - \dot{\alpha}_c) - \tilde{\gamma}\left(\bar{q}SC_{L_\alpha}/mV\right) - \left(\epsilon_{L_1}/mV\right) \tag{27}$$

$$\dot{\tilde{Q}} = -K_Q\tilde{Q} + (\dot{\tilde{Q}}_c - \dot{Q}_c) + \nu_Q - \tilde{\alpha} + c_7\epsilon_{M_1} \tag{28}$$

$$\dot{\tilde{V}} = -K_v\tilde{V} + \nu_V - \left(\epsilon_{D_1}/m\right) \tag{29}$$

Define a Lyapunov function as

$$\mathcal{V}_{(\gamma,\alpha,Q,V)} = \tfrac{1}{2}(\tilde{\gamma}^2 + \tilde{\alpha}^2 + \tilde{Q}^2 + \tilde{V}^2)$$

The derivative of $\mathcal{V}$ along solutions of the γ, α, Q, and V tracking error dynamic equations is

$$\dot{\mathcal{V}}_{(\gamma,\alpha,Q,V)} = -\left(K_\gamma\tilde{\gamma}^2 + K_\alpha\tilde{\alpha}^2 + K_Q\tilde{Q}^2 + K_V\tilde{V}^2\right) + \nu_\gamma\tilde{\gamma} + \nu_\alpha\tilde{\alpha} + \nu_Q\tilde{Q} + \nu_V\tilde{V} + (\tilde{\gamma} - \tilde{\alpha})\left(\epsilon_{L_1}/mV\right) + \tilde{\alpha}(\dot{\tilde{\alpha}}_c - \dot{\alpha}_c) + \tilde{Q}(\dot{\tilde{Q}}_c - \dot{Q}_c) + \tilde{Q}c_7\epsilon_{M_1} - \tilde{V}\left(\epsilon_{D_1}/m\right) \tag{30}$$

At this point, analysis similar to that of Appendix A could be used to analyze the stability of this backstepping controller. We do not

include that analysis herein because such a result would be very similar to a result proved later, that is, Theorem 2. The main goal of this section is to introduce equations and ideas that will be built on in subsequent sections. Note that for a well-modeled system each of the terms ϵ_{L_1}/mV, $[\dot{\bar{\alpha}}_c - \dot{\alpha}_c - (\epsilon_{L_1}/mV)]$, $(\dot{\bar{Q}}_c - \dot{Q}_c + c_7\epsilon_{M_1})$, and ϵ_{D_1}/m would be quite small; however, modeling error, possibly due to in-flight changes in the aircraft, will excite tracking error to possibly unacceptable limits. The challenge, as addressed in the next section, is to ensure that the system is well modeled, even when in-flight events change the vehicle dynamics. This will be achieved without resorting to high control gains.

D. Backstepping Control of γ, α, Q, and V: Unknown Aerodynamic Functions

The preceding analysis was based on exact knowledge of the coefficient functions. Now, we consider the case where the functions C_L, C_{L_α}, C_D, $C_{D_{\delta_i}}$, C_{M_o}, C_{M_Q}, and $C_{M_{\delta_i}}$ are unknown and are approximated online.

1. *Coefficient Approximator Definition*

The online approximations to the aerodynamic coefficient functions are given by Eqs. (8–10) and

$$\hat{C}_L = \theta_{C_L}^T \phi(\boldsymbol{x}_r), \qquad \hat{C}_{L_\alpha} = \theta_{C_{L_\alpha}}^T \phi(\boldsymbol{x}_r) \tag{31}$$

$$\hat{C}_D(x_r) = \theta_D^T \phi(\boldsymbol{x}_r), \qquad \hat{C}_{D_{\delta_i}}(x_r) = \theta_{D_{\delta_i}} \phi(\boldsymbol{x}_r) \tag{32}$$

where different basis vectors ϕ and arguments $\boldsymbol{x}_r$ could be used for each coefficient function, but this is not done herein solely for convenience of notation.

By analysis similar to that in Sec. II.D, we define the optimal lift approximation parameters and minimum uniform approximation error for the selected basis set as

$$\Theta_L^* = \operatorname{argmin}_{\Theta_L} \left\{ \sup_{x_r \in \mathcal{D}} \left| \left[(C_L(\boldsymbol{x}_r) + C_{L_\alpha}(\boldsymbol{x}_r)\alpha \right] - \left(\theta_L^T + \theta_{L_\alpha}^T \alpha\right)\phi(\boldsymbol{x}_r) \right| \right\} \tag{33}$$

$$\epsilon_{L_2}(\boldsymbol{x}_r) = \left[C_L(\boldsymbol{x}_r) + C_{L_\alpha}(\boldsymbol{x}_r)\alpha \right] - \left(\theta_L^T + \theta_{L_\alpha}^T \alpha\right)\Big|_{\Theta_L^*} \phi(\boldsymbol{x}_r) \tag{34}$$

$$\bar{\epsilon}_{L_2} = \sup_{x_r \in \mathcal{D}} \left| \epsilon_{L_2}(\boldsymbol{x}_r) \right| \tag{35}$$

where $\Theta_L = [\theta_L, \theta_{L_\alpha}]$. If $\mathcal{D}$ is compact and L is continuous, then the bound $\bar{\epsilon}_{L_2}$ is well defined and small for appropriate selection of the basis vector $\phi(\boldsymbol{x}_r)$. Therefore,

$$\left[C_L(\boldsymbol{x}_r) + C_{L_\alpha}(\boldsymbol{x}_r)\alpha \right] = \left[\theta_L^T \phi(\boldsymbol{x}_r) + \theta_{L_\alpha}^T \phi(\boldsymbol{x}_r)\alpha \right] - \left[\tilde{\theta}_L^T \phi(\boldsymbol{x}_r) + \tilde{\theta}_{L_\alpha}^T \phi(\boldsymbol{x}_r)\alpha \right] + \epsilon_{L_2}(\boldsymbol{x}_r) \tag{36}$$

where $\tilde{\theta}_L = \theta_L - \theta_L^*$ and $\tilde{\theta}_{L_\alpha} = \theta_{L_\alpha} - \theta_{L_\alpha}^*$. Note that θ_L^*, $\theta_{L_\alpha}^*$, and $\epsilon_{L_2}(\boldsymbol{x}_r)$ are used only for analysis and are not needed for implementation of the control law.

Similarly we define the optimal drag approximation parameters and minimal uniform drag approximation error for the selected basis set as

$$\Theta_D^* = \operatorname{argmin}_{\Theta_D} \left\{ \sup_{x_r \in \mathcal{D}} \left| \left[C_D(\boldsymbol{x}_r) + \sum_{i=1}^{m} C_{D_{\delta_i}}(\boldsymbol{x}_r)|\delta_i| \right] - \left(\theta_D^T + \sum_{i=1}^{m} \theta_{D_{\delta_i}}^T |\boldsymbol{\delta}_i| \right) \phi(\boldsymbol{x}_r) \right| \right\} \tag{37}$$

$$\epsilon_{D_2}(x_r) = \left[C_D(\boldsymbol{x}_r) + \sum_{i=1}^{m} C_{D_{\delta_i}}(\boldsymbol{x}_r)|\delta_i| \right] - \left(\theta_D^T + \sum_{i=1}^{m} \theta_{D_{\delta_i}}^T |\boldsymbol{\delta}_i| \right)\Big|_{\Theta_D^*} \phi(\boldsymbol{x}_r) \tag{38}$$

$$\bar{\epsilon}_{D_2} = \sup_{x_r \in \mathcal{D}} \left| \epsilon_{D_2}(\boldsymbol{x}_r) \right| \tag{39}$$

where $\Theta_D = [\theta_D, \theta_{D_{\delta_1}}, \ldots, \theta_{D_{\delta_1}}]$. If $\mathcal{D}$ is compact and D is continuous, then Θ_D^*, $\epsilon_{D_2}(\boldsymbol{x}_r)$, and $\bar{\epsilon}_{D_2}$ are well defined and bounded. The bound $\bar{\epsilon}_{D_2}$ is small for appropriate selection of the basis vector $\phi(\boldsymbol{x}_r)$. Therefore,

$$C_D(x_r) + \sum_{i=1}^{m} C_{D_{\delta_i}}(\boldsymbol{x}_r)|\boldsymbol{\delta}_i| = \left(\theta_D^T + \sum_{i=1}^{m} \theta_{D_{\delta_i}}^T |\boldsymbol{\delta}_i| \right) \phi(\boldsymbol{x}_r) - \left(\tilde{\theta}_D^T + \sum_{i=1}^{m} \tilde{\theta}_{D_{\delta_i}}^T |\boldsymbol{\delta}_i| \right) \phi(\boldsymbol{x}_r) + \epsilon_{D_2}(\boldsymbol{x}_r) \tag{40}$$

where $\tilde{\theta}_D = \theta_D - \theta_D^*$ and $\tilde{\theta}_{D_{\delta_i}} = \theta_{D_{\delta_i}} - \theta_{D_{\delta_i}}^*$. Note that θ_D^*, $\theta_{D_{\delta_i}}^*$, and $\epsilon_{D_2}(\boldsymbol{x}_r)$ are used only for analysis and are not needed for implementation of the control law.

In the following, the argument $(\boldsymbol{x}_r)$ of ϕ and each of the coefficient functions are dropped.

2. *Online Approximation Based Control Law*

Since the unknown aerodynamic coefficients are approximated online, for each of the control signals of Eqs. (22–25) replace the unknown functions by their approximations in the specified control law

$$\alpha_c = \frac{1}{\hat{C}_{L_\alpha}} \left[-\hat{C}_L + \frac{mV}{\bar{q}S}(-f_\gamma + \dot{\gamma}_c - K_\gamma \tilde{\gamma} + \nu_\gamma) \right] \tag{41}$$

$$Q_c = \frac{\bar{q}S\left(\hat{C}_L + \hat{C}_{L_\alpha}\alpha\right)}{mV} - K_\alpha \tilde{\alpha} + f_\alpha + \dot{\bar{\alpha}}_c + \nu_\alpha - \tilde{\gamma}\frac{\bar{q}S\hat{C}_{L_\alpha}}{mV} \tag{42}$$

$$u_Q = -\bar{q}S\bar{c}\left(\hat{C}_{M_o} + \hat{C}_{M_Q}\frac{\bar{c}Q}{2V} \right) \frac{-k_Q\tilde{Q} + \nu_Q - \tilde{\alpha} + \dot{\bar{Q}}_c - f_Q}{c_7} \tag{43}$$

$$T = \left\{ \bar{q}S\left(\hat{C}_D + \sum_{i=1}^{m} \hat{C}_{D_{\delta i}}|\delta_i| \right) + mg\sin(\gamma) + m[\dot{V}_c - K_v(V - V_c) + \nu_V] \right\} \Big/ \cos(\alpha) \tag{44}$$

Then, with the online approximations, the controlled tracking error dynamics are

$$\dot{\tilde{\gamma}} = -K_\gamma\,\tilde{\gamma} + \nu_\gamma + \tilde{\alpha}\frac{\bar{q}S\hat{C}_{L_\alpha}}{mV} - \frac{\bar{q}S}{mV}\left(\tilde{\theta}_L^T\phi + \tilde{\theta}_{L_\alpha}^T\phi\alpha\right) + \frac{\left(\epsilon_{L_1} + \bar{q}S\epsilon_{L_2}\right)}{mV} \tag{45}$$

$$\dot{\tilde{\alpha}} = -K_\alpha\tilde{\alpha} + \nu_\alpha + \tilde{Q} - \tilde{\gamma}\frac{\bar{q}S\hat{C}_{L_\alpha}}{mV} + \frac{\bar{q}S}{mV}\left(\tilde{\theta}_L^T\phi + \tilde{\theta}_{L_\alpha}^T\phi\alpha\right) - \frac{\left(\epsilon_{L_1} + \bar{q}S\epsilon_{L_2}\right)}{mV} + (\dot{\bar{\alpha}}_c - \dot{\alpha}_c) \tag{46}$$

$$\dot{\tilde{Q}} = -k_Q \tilde{Q} + \nu_Q - \tilde{\alpha} - c_7 \bar{q} S \bar{c} \left[\left(\tilde{\theta}_{M_o}^T + \tilde{\theta}_{M_Q}^T \frac{\bar{c} Q}{2V} + \sum_{i=1}^{m} \tilde{\theta}_{M_{\delta_i}}^T \delta_i \right) \phi \right] + c_7 \left[\epsilon_{M_2} + \epsilon_{M_1} \right] + (\dot{\tilde{Q}}_c - \dot{Q}_c) \tag{47}$$

$$\dot{\tilde{V}} = -K_v \tilde{V} + \nu_V + \frac{\bar{q} S}{m} \left(\tilde{\theta}_D^T \phi + \sum_{i=1}^{m} \tilde{\theta}_{D_{\delta_i}}^T \phi |\delta_i| \right) - \epsilon_{D_1} - \bar{q} S \epsilon_{D_2} \tag{48}$$

The remaining issues are specification of the parameter adaptation laws and analysis of the stability properties of the online approximation-basedcontrol law. These issues are addressed in the following section.

3. *Stability Analysis and Parameter Adaptation*

This section will analyze the (γ, α, Q) and V controlled tracking error dynamics separately. This separation is purely for convenience of presentation. We use the fact that if $\mathcal{V}_{(\gamma,\alpha,Q)}$ is positive definite in (γ, α, Q) and the lift and moment parameters, and $\mathcal{V}_V$ is positive definite in V and the drag parameters, then $\mathcal{V} = \mathcal{V}_{(\gamma,\alpha,Q)} + \mathcal{V}_V$ is positive definite in (γ, α, Q, V) and the lift, drag, and moment parameters.

Parameter adaptation and stability analysis for airspeed. Consider the Lyapunov function

$$\mathcal{V}_V = \frac{1}{2} \left(\tilde{V}^2 + \tilde{\theta}_D^T \Gamma_D^{-1} \tilde{\theta}_D + \sum_{i=1}^{m} \tilde{\theta}_{D_{\delta_i}}^T \Gamma_{D_{\delta_i}}^{-1} \tilde{\theta}_{D_{\delta_i}} \right) \tag{49}$$

and let the drag coefficient parameters adapt according to

$$\dot{\tilde{\theta}}_D = \dot{\theta}_D = -\Gamma_D (\bar{q} S / m) \tilde{V} \phi \tag{50}$$

$$\dot{\tilde{\theta}}_{D_{\delta_i}} = \dot{\theta}_{D_{\delta_i}} = -\Gamma_{D_{\delta_i}} (\bar{q} S / m) \tilde{V} \phi |\delta_i| \tag{51}$$

for $K_V |\tilde{V}| > (\epsilon_{D_1} + \bar{q} S \epsilon_{D_2})$, where Γ_D and $\Gamma_{D_{\delta_i}}$ are symmetric and positive definite parameter adaptation gain matrices.

The derivative of this Lyapunov function along solutions of Eq. (48), for $K_V |\tilde{V}| > (\epsilon_{D_1} + \bar{q} S \epsilon_{D_2})$, is

$$\dot{\mathcal{V}}_V = -K_v \tilde{V}^2 + \nu_V \tilde{V} - \left(\epsilon_{D_1} + \bar{q} S \epsilon_{D_2} \right) \tilde{V} \tag{52}$$

If ν_V is selected such that $\nu_V \tilde{V} \le 0$ and $|\nu_V| \ge |\epsilon_{D_1} + \bar{q} S \epsilon_{D_2}|$, then $\dot{\mathcal{V}}_V$ is negative semidefinite and asymptotic stability can be proved; however, satisfaction of these requirements usually requires a discontinuous ν_V (e.g., $\nu_V = -K \operatorname{sign}(\tilde{V})$ for $K > 0$ and sufficiently large), which is not desirable. Even with $\nu_V = 0$, Eq. (52) is negative semidefinite for $K_v |\tilde{V}| > (\epsilon_{D_1} + \bar{q} S \epsilon_{D_2})$. Following the analysis of Appendix A, it is possible to show that $\tilde{V}, \tilde{\theta}_D, \dot{\tilde{\theta}}_D, \tilde{\theta}_{D_{\delta_i}}, \dot{\tilde{\theta}}_{D_{\delta_i}} \in \mathcal{L}_\infty$ and that $\tilde{V}$ is r^2 small in the MSS where $r^2 = (1/K_v^2)(\epsilon_{D_1} + \bar{q} S \epsilon_{D_2})^2$. If ν_V is selected such that $\tilde{V} \nu_V \le 0$ (e.g., $\nu_V = -K(\tilde{V})^3$ for $K > 0$), then the bounds of the preceding sentence are decreased.

Parameter adaptation and stability analysis for (γ, α, Q). Define the (γ, α, Q) Lyapunov function as

$$\mathcal{V}_{(\gamma,\alpha,Q)} = \frac{1}{2} \left(\tilde{\gamma}^2 + \tilde{\alpha}^2 + \tilde{Q}^2 + \tilde{\theta}_L^T \Gamma_L^{-1} \tilde{\theta}_L + \tilde{\theta}_{L_\alpha}^T \Gamma_{L_\alpha}^{-1} \tilde{\theta}_{L_\alpha} \right) + \frac{1}{2} \left(\tilde{\theta}_M^T \Gamma_{M_o}^{-1} \tilde{\theta}_{M_o} + \tilde{\theta}_{M_Q}^T \Gamma_{M_Q}^{-1} \tilde{\theta}_{M_Q} + \sum_{i=1}^{m} \tilde{\theta}_{M_{\delta_i}}^T \Gamma_{M_{\delta_i}}^{-1} \tilde{\theta}_{M_{\delta_i}} \right)$$

where Γ_L, Γ_{L_α}, Γ_{M_o}, Γ_{M_Q}, and $\Gamma_{M_{\delta_i}}$ are positive definite and symmetric parameter adaptation gain matrices. Let the lift and moment coefficient parameters adapt according to

$$\dot{\theta}_{C_L} = \Gamma_L (\bar{q} S / mV)(\tilde{\gamma} - \tilde{\alpha}) \phi \tag{53}$$

$$\dot{\theta}_{C_{L_\alpha}} = \Gamma_{L_\alpha} (\bar{q} S / mV)(\tilde{\gamma} - \tilde{\alpha}) \phi \alpha \tag{54}$$

$$\dot{\theta}_{M_o} = \Gamma_{M_o} c_7 (\bar{q} S \bar{c}) \tilde{Q} \phi \tag{55}$$

$$\dot{\theta}_{M_Q} = \Gamma_{M_Q} c_7 (\bar{q} S \bar{c}) \tilde{Q} \phi (\bar{c} Q / 2V) \tag{56}$$

$$\dot{\theta}_{M_{\delta i}} = \Gamma_{M_{\delta_i}} c_7 (\bar{q} S \bar{c}) \tilde{Q} \phi \delta_i, \qquad i = 1, \ldots, m \tag{57}$$

for

$$|\tilde{\gamma}| > \frac{1}{K_\gamma} \left| \frac{(\bar{\epsilon}_{L_1} + \bar{q} S \bar{\epsilon}_{L_2})}{mV} \right|$$

$$|\tilde{\alpha}| > \frac{1}{K_\alpha} \left| (\dot{\tilde{\alpha}}_c - \dot{\alpha}_c) - \frac{\left(\bar{\epsilon}_{L_1} + \bar{q} S \bar{\epsilon}_{L_2} \right)}{mV} \right|$$

$$|\tilde{Q}| > \frac{1}{K_Q} \left| c_7 \left[\epsilon_{M_2} + \epsilon_{M_1} \right] + (\dot{\tilde{Q}}_c - \dot{Q}_c) \right|$$

where $\bar{\epsilon}_{L_1}$ and $\bar{\epsilon}_{L_2}$ are upper bounds on ϵ_{L_1} and ϵ_{L_2}. When

$$|\tilde{\gamma}| < \frac{1}{K_\gamma} \left| \frac{(\bar{\epsilon}_{L_1} + \bar{q} S \bar{\epsilon}_{L_2})}{mV} \right|$$

or

$$|\tilde{\alpha}| < \frac{1}{K_\alpha} \left| (\dot{\tilde{\alpha}}_c - \dot{\alpha}_c) + \frac{(\bar{\epsilon}_{L_1} + \bar{q} S \bar{\epsilon}_{L_2})}{mV} \right|$$

then $\dot{\theta}_{C_L} = 0$ and $\dot{\theta}_{C_{L_\alpha}} = 0$. When

$$|\tilde{Q}| < (1/K_Q) \left| c_7 \left[\epsilon_{M_2} + \epsilon_{M_1} \right] + (\dot{\tilde{Q}}_c - \dot{Q}_c) \right|$$

then $\dot{\theta}_{M_o} = 0$, $\dot{\theta}_{M_Q} = 0$, and $\dot{\theta}_{M_{\delta i}} = 0$.

The derivative of $\mathcal{V}_{(\gamma,\alpha,Q)}$ along solutions of the (γ, α, Q) controlled tracking error dynamic equations with the parameter update laws defined by Eqs. (53–57) is

$$\dot{\mathcal{V}}_{(\gamma,\alpha,Q)} = -\left(K_\gamma \tilde{\gamma}^2 + K_\alpha \tilde{\alpha}^2 + k_Q \tilde{Q}^2 \right) + \nu_\gamma \tilde{\gamma} + \nu_\alpha \tilde{\alpha} + \nu_Q \tilde{Q} + \epsilon \tag{58}$$

where

$$\epsilon = \tilde{\alpha} (\dot{\tilde{\alpha}}_c - \dot{\alpha}_c) + (\tilde{\gamma} - \tilde{\alpha}) \left[\left(\epsilon_{L_1} + \bar{q} S \epsilon_{L_2} \right) / mV \right] + c_7 \left[\epsilon_{M_2} + \epsilon_{M_1} \right] \tilde{Q} + (\dot{\tilde{Q}}_c - \dot{Q}_c) \tilde{Q}$$

Therefore, for $(K_\gamma, K_\alpha, k_Q)$ positive:

1) If $(\dot{\tilde{\alpha}}_c - \dot{\alpha}_c) = (\dot{\tilde{Q}}_c - \dot{Q}_c) = \epsilon_{M_1} = \epsilon_{M_2} = \epsilon_{L_1} = \epsilon_{L_2} = 0$, then even for $\nu_\gamma = \nu_\alpha = \nu_Q = 0$ we have $\mathcal{V}_{(\gamma,\alpha,Q)}$ negative semidefinite, which implies [by Barbalat's lemma, (see Ref. 22, p. 122)] that each tracking error is asymptotically stable.

2) If ν_γ has sign opposite to $\tilde{\gamma}$ and magnitude larger than $|(\epsilon_{L_1} + \bar{q} S \epsilon_{L_2})/mV|$, ν_α has sign opposite to $\tilde{\alpha}$ and magnitude greater than $|\dot{\tilde{\alpha}}_c - \dot{\alpha}_c - [(\epsilon_{L_1} + \bar{q} S \epsilon_{L_2})/mV]|$, and ν_Q has sign opposite to $\tilde{Q}$ and magnitude larger than $|\dot{\tilde{Q}}_c - \dot{Q}_c + c_7(\epsilon_{M_1} + \epsilon_{M_2})|$, then $\dot{\mathcal{V}}_{(\gamma,\alpha,Q)}$ is negative semidefinite. Therefore, by Barbalat's lemma, the tracking error is asymptotically stable.

3) If each of the terms ϵ_{L_1}/mV, $\bar{q} S (\epsilon_{L_2}/mV)$, $(\dot{\tilde{\alpha}}_c - \dot{\alpha}_c)$, $(\dot{\tilde{Q}}_c - \dot{Q}_c)$, and $[c_7(\epsilon_{M_1} + \epsilon_{M_2})]$ is bounded, then the tracking error is uniformly ultimately bounded. Each of these terms should be small for a properly designed system. Following the approach of Appendix A, it can be shown that $\tilde{\gamma}, \tilde{\alpha}, \tilde{Q}, \tilde{\Theta}, \dot{\tilde{\Theta}} \in \mathcal{L}_\infty$ and that the

signals $\tilde{\gamma}$, $\tilde{\alpha}$, and $\tilde{Q}$ are each s^2 small in the MSS, where

$$s^2 = \frac{1}{K_\gamma}\left(\frac{\epsilon_{L_1} + \bar{q}S\epsilon_{L_2}}{mV}\right)^2 + \frac{1}{K_\alpha}\left(\dot{\tilde{\alpha}}_c - \dot{\alpha}_c - \frac{\epsilon_{L_1} + \bar{q}S\epsilon_{L_2}}{mV}\right)^2 + \frac{1}{K_Q}\left[c_7\left(\epsilon_{M_2} + \epsilon_{M_1}\right) + (\dot{\tilde{Q}}_c - \dot{Q}_c)\right]^2$$

If ν_γ has sign opposite to $\tilde{\gamma}$, ν_α has sign opposite to $\tilde{\alpha}$, and ν_Q has sign opposite to $\tilde{Q}$, then the magnitude of this bound is decreased.

The third case will be the case that holds in most applications. Although it is possible to decrease s^2 by increasing K_γ, K_α, and K_Q, this is not a desirable approach because these parameters determine the closed-loop bandwidth. Also, the designer can force the second case by selecting $\nu_\gamma = -K_1\,\mathrm{sign}(\tilde{\gamma})$, $\nu_\alpha = -K_2\,\mathrm{sign}(\tilde{\alpha})$, $\nu_Q = -K_3\,\mathrm{sign}(\tilde{Q})$ with K_1, K_2, K_3 sufficiently large, but this will cause the control signals to be discontinuous, which is not desirable. Case three is preferred because s is small.

E. Outer-Loop Control Law Summary

The equations of the online approximation-based controller follow:

$$\alpha_c = \left(1/\hat{C}_{L_\alpha}\right)\left[-\hat{C}_L + (mV/\bar{q}S)(-f_\gamma + \dot{\gamma}_c - K_\gamma\tilde{\gamma} + \nu_\gamma)\right]$$

$$Q_c = \bar{q}S\left(\hat{C}_L + \hat{C}_{L_\alpha}\alpha\right)/mV - K_\alpha\tilde{\alpha} + f_\gamma + \dot{\alpha}_c + \nu_\alpha - \tilde{\gamma}\left(\bar{q}S\hat{C}_{L_\alpha}/mV\right)$$

$$\hat{u}_Q = -\bar{q}S\bar{c}\left[\hat{C}_{M_o} + \hat{C}_{M_Q}(\bar{c}Q/2V)\right] + (1/c_7)(-K_Q\tilde{Q} + \dot{\tilde{Q}}_c + \nu_Q - \tilde{\alpha} - f_Q)$$

$$T = \frac{1}{\cos(\alpha)}\left\{\bar{q}S\left(\hat{C}_D + \sum_{i=1}^{m}\hat{C}_{D_{\delta i}}\delta_i\right) + m[\dot{V}_c - K_v(V - V_c) + g\sin(\gamma)]\right\}$$

Select $\boldsymbol{\delta}$ such that $\hat{u}_Q = \hat{G}_Q\boldsymbol{\delta}$, where

$$\hat{G}_Q = \bar{q}S\bar{c}\left[\hat{C}_{M_{\delta_1}}, \ldots, \hat{C}_{M_{\delta m}}\right]^T$$

The coefficients are

$$\hat{C}_{L_o} = \theta_{L_o}^T\phi(\boldsymbol{x}_r), \qquad \hat{C}_{L_\alpha} = \theta_{L_\alpha}^T\phi(\boldsymbol{x}_r)$$

$$\hat{C}_D = \theta_D^T\phi(\boldsymbol{x}_r), \qquad \hat{C}_{D_{\delta_i}} = \theta_{D_{\delta_i}}^T\phi(\boldsymbol{x}_r)$$

$$\hat{C}_{M_o} = \theta_{M_o}^T\phi(\boldsymbol{x}_r), \qquad \hat{C}_{M_Q} = \theta_{M_Q}^T\phi(\boldsymbol{x}_r)$$

$$\hat{C}_{M_{\delta_i}} = \theta_{M_{\delta_i}}^T\phi(\boldsymbol{x}_r)$$

The parameter adaptation equations are specified in Eqs. (50), (51), and (53–57). The index $i \in [1, m]$. The properties of this controller are summarized in Theorem 2.

Theorem 2: The control law summarized in the preceding equations stabilizes the (γ, α, Q, V) dynamics of an aircraft in the sense that 1) $(\tilde{\gamma}, \tilde{\alpha}, \tilde{Q}, \tilde{V})$ are each ultimately bounded by

$$|\tilde{\gamma}| \le \frac{1}{K_\gamma}\left|\frac{\epsilon_{L_1} + \bar{q}S\epsilon_{L_2}}{mV}\right|$$

$$|\tilde{\alpha}| \le \frac{1}{K_\alpha}\left|\left[(\dot{\tilde{\alpha}}_c - \dot{\alpha}_c) - \frac{\left(\epsilon_{L_1} + \bar{q}S\epsilon_{L_2}\right)}{mV}\right]\right|$$

$$|\tilde{Q}| \le \frac{1}{K_Q}\left|c_7\left[\epsilon_{M_2} + \epsilon_{M_1}\right] + (\dot{\tilde{Q}}_c - \dot{Q}_c)\right|$$

$$|\tilde{V}| \le \frac{1}{K_v}\left|\epsilon_{D_1} + \bar{q}S\epsilon_{D_2}\right|$$

2) $\tilde{\gamma}$, $\tilde{\alpha}$, $\tilde{Q}$, $\tilde{V}$, $\tilde{\Theta}$, $\dot{\tilde{\Theta}} \in \mathcal{L}_\infty$; 3) $\tilde{V}$ is r^2 small in the MSS, where $r = (1/K_v)(\epsilon_{D_1} + \bar{q}S\epsilon_{D_2})$; and 4) $K_\gamma\tilde{\gamma} + K_\alpha\tilde{\alpha} + K_Q\tilde{Q}$ is s^2 small in the MSS, where

$$s^2 = \frac{1}{K_\gamma}\left(\frac{\epsilon_{L_1} + \bar{q}S\epsilon_{L_2}}{mV}\right)^2 + \frac{1}{K_\alpha}\left(\dot{\tilde{\alpha}}_c - \dot{\alpha}_c - \frac{\epsilon_{L_1} + \bar{q}S\epsilon_{L_2}}{mV}\right)^2 + \frac{1}{K_Q}\left[c_7\left(\epsilon_{M_2} + \epsilon_{M_1}\right) + (\dot{\tilde{Q}}_c - \dot{Q}_c)\right]^2$$

where $(\tilde{\gamma}, \tilde{\alpha}, \tilde{Q}, \tilde{V}) = (\gamma - \gamma_c, \alpha - \alpha_c, Q - Q_c, V - V_c)$ and $\Theta = [\Theta_L, \theta_{L_\alpha}, \Theta_D, \Theta_{D_{\delta_i}}, \Theta_M]$, for $i = 1, \ldots, m$. All other terms are defined in the Nomenclature.

IV. Simulation Analysis

The preceding sections have presented the theory for the design of an approximation-based backstepping controller. This section presents simulation results for the controller summarized in Sec. III.E. The controller parameters are

$$K_\gamma = 0.3, \qquad K_\alpha = 3, \qquad K_Q = 30$$

$$K_V = 0.2, \qquad \nu_\gamma = -(10\tilde{\gamma})^3, \qquad \nu_\alpha = -(10\tilde{\alpha})^3$$

$$\nu_Q = 0, \qquad \nu_V = 0$$

where $\tilde{\gamma}$ and $\tilde{\alpha}$ are in radians; K_γ, K_α, K_Q, K_V, ν_γ, and ν_α have units of s^{-1}; ν_Q has units of s^{-2}; and ν_V has units of $\mathrm{ft/s}^2$. Issues related to the selection of the controller parameters are discussed further in Sec. IV.B. The vehicle for these simulations is a tailless uninhabited combat air vehicle with one engine and six control surfaces, that is, δ_1 = right outer flap, δ_2 = left outer flap, δ_3 = right midflap, δ_4 = left midflap, δ_5 = right spoiler, and δ_6 = left spoiler. The spoilers are directly in front of the midflaps. Therefore, the midflap effectiveness is a function of the spoiler deflection. The spoiler deflection is restricted to be positive. The nonlinear aircraft simulation incorporates second-order actuator models with magnitude and rate limit constraints. The thrust model includes first-order rate limited dynamics with magnitude limited to the range [100, 5000] lb (or [444, 22,241] N). When the thrust command is at its lower limit, the airspeed controller deflects the spoilers to create the necessary drag to cause the vehicle to track the commanded speed. Given these constraints, the simulation selects the surface deflections according to

$$\boldsymbol{\delta} = \boldsymbol{d} + W^{-1}\hat{G}_Q^T\left[\hat{G}_Q W^{-1}\hat{G}_Q^T\right]^{-1}(\hat{u}_Q - \hat{G}_Q\boldsymbol{d}) \tag{59}$$

where W is a positive definite matrix and $\boldsymbol{d} \in \Re^6$ is a possibly time-varying vector.[37] This actuator distribution approach minimizes $(\boldsymbol{\delta} - \boldsymbol{d})^T W(\boldsymbol{\delta} - \boldsymbol{d})$ subject to the constraint that $\hat{u}_Q = \hat{G}_Q\boldsymbol{\delta}$. The time step for the numeric simulation is 0.01 s. The open-loop vehicle is unstable.

As summarized in the coefficients listed in Sec. III.E, 17 functions will be approximated. For all functions except $C_{M_{\delta_3}}$ and $C_{M_{\delta_4}}$, the regressor argument is $\boldsymbol{x}_r = (\alpha, M)$. For $C_{M_{\delta_3}}$, the regressor argument is $\boldsymbol{x}_r = (\alpha, M, \delta_5)$. For $C_{M_{\delta_4}}$, the regressor argument is $\boldsymbol{x}_r = (\alpha, M, \delta_6)$. Each element of the regressor vector $\phi(\boldsymbol{x}_r)$ is implemented as third-order B spline.[43] The spline and online approximation implementation are designed so that significantly fewer than N regressor elements and model parameters are computed at each iteration. This is achieved by defining the B-spline knots on a grid. This greatly decreases the computational load. The spline knots for α are spaced every 2 deg between −8 and 20 deg. The spline knots for M are spaced every 0.2 units between 0.0 and 1.0. The spline knots for spoiler deflection are spaced every 10 deg between 0.0 and 60.

At $t = 0$, the vehicle is flying $V = 300$ fps with an altitude of 5000 ft, when an event occurs that changes the aircraft dynamics.

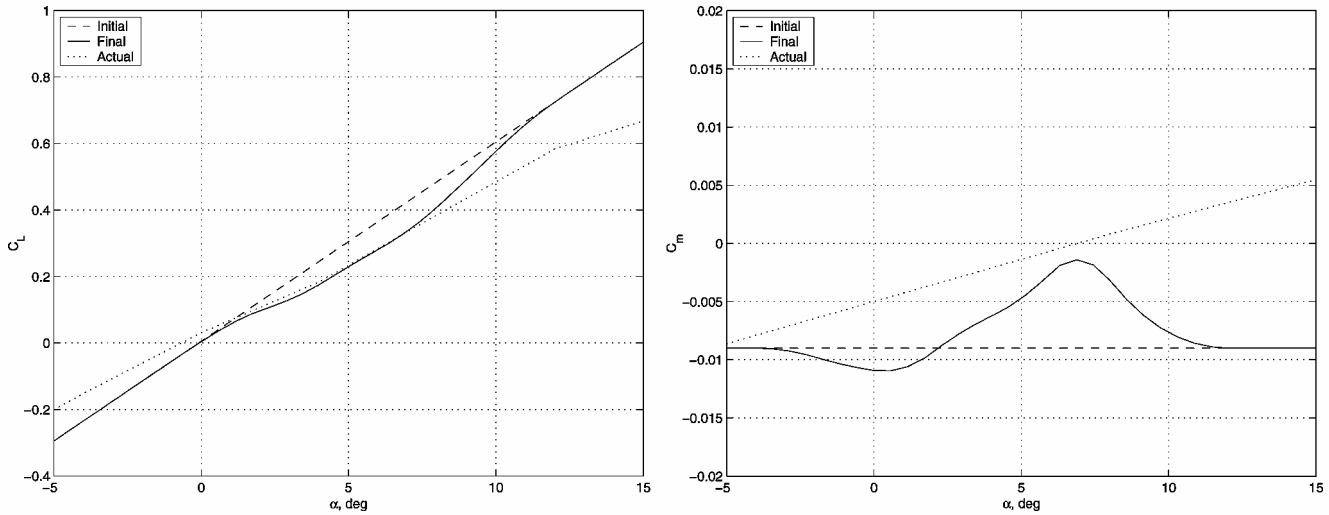

Fig. 2 Functions: . . . . , actual aerodynamic functions $C_{M_o}(x_r)$ and $C_{L_o}(x_r) + C_{L_\alpha}(x_r)\alpha$ vs alpha; – – –, approximations to these functions at beginning of simulation; and ——, approximations to these functions at end of simulation.

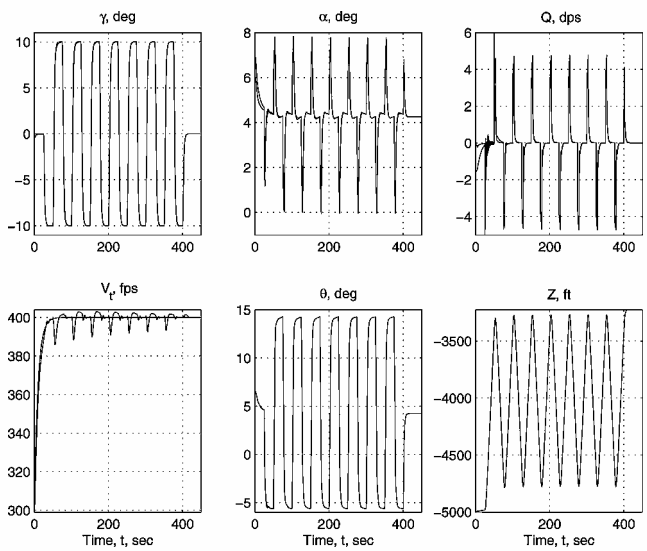

Fig. 3 Time series of commanded and actual longitudinal states of the aircraft, that is, two curves per subplot. Simulation starts with all coefficients of aerodynamics model incorrect.

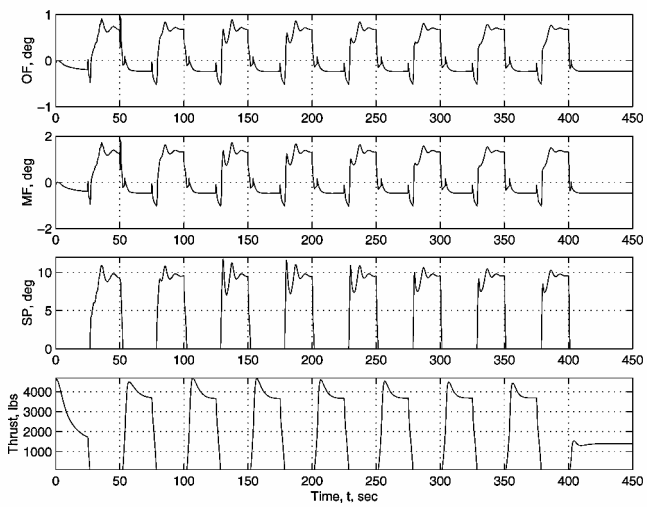

Fig. 4 Surface positions and thrust commands required to execute the state trajectory shown in Fig. 3.

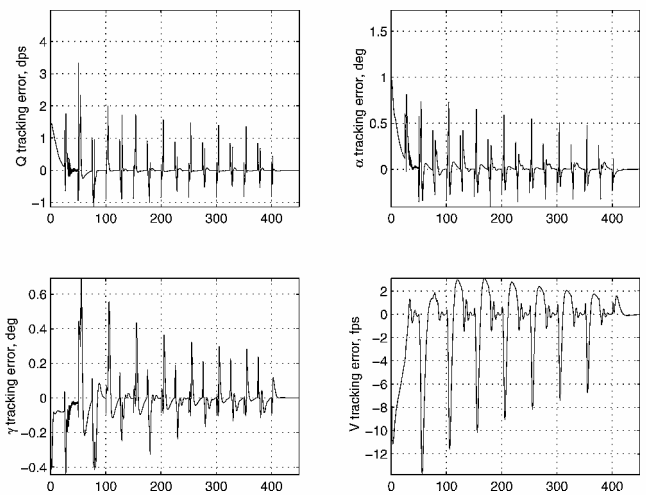

Fig. 5 Time series of command tracking errors for the longitudinal states with parameter adaptation on. Compare with Fig. 7.

Therefore, all of the aerodynamic coefficient functions in the controller become incorrect. Figure 2 shows the actual coefficient of lift and coefficient of moment functions compared to the controller approximations to the same functions at the start and end of the simulation. Figures 3–6 show information for a simulation evaluation of the online approximation-based backstepping controller performance. The commanded and actual state trajectories are shown in Fig. 3 for the subsequent 450 s. During this period of time, the vehicle speed is commanded to 400 fps, and starting at $t = 25$ s, the gamma command is a series of 10-deg doublets with a period of 50 s. The gamma doublets are prefiltered by a first-order filter with a pole at $s = -0.5$ and a 5 deg/s rate limit. This prefilter provides $\dot{\gamma}_c$ and a continuous γ_c. The γ and V commands are inputs to the online approximation-based backstepping controller. The α_c and Q_c signals are generated within the control law by Eqs. (41) and (42). The actuator signals are shown in Fig. 4. The time series for the tracking errors are shown in Fig. 5. To compare the tracking errors for repetitions of the same portion of the command more easily, Fig. 6 shows the first 20 s of the tracking errors following $t = 50$, 150, 250, and 350 s redrawn from Fig. 5 to allow more direct comparison of the change in tracking performance between comparable portions of the trajectory. At each of these times, the signal γ_c has just switched from -10 to 10 deg. Note that the tracking errors are small, they converge toward zero during each doublet, and the peak errors between repetitions of doublets is decreasing. Also, the

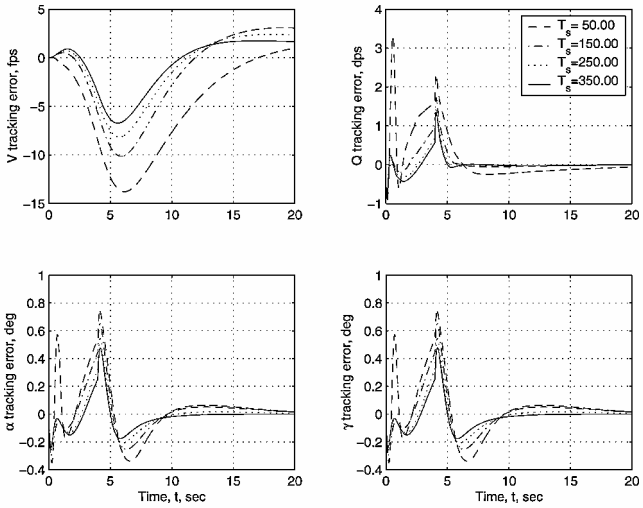

Fig. 6 First 20 s of transients to γ commands starting at $t = 50$, 150, 250, and 350 s.

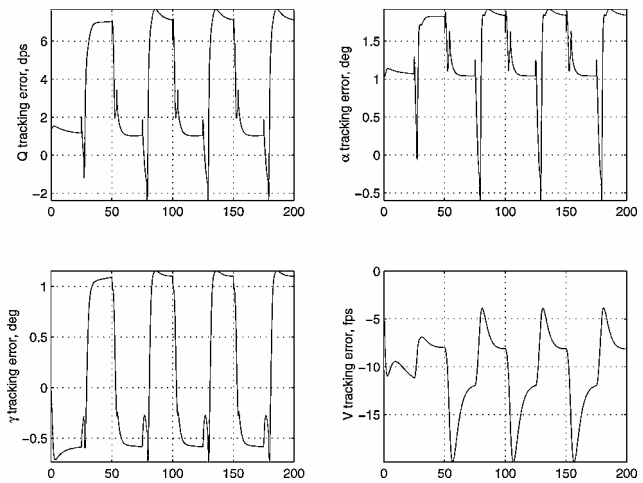

Fig. 7 Time series of command tracking errors for longitudinal states with the parameter adaptation turned off.

energy, that is, integrated squared error, of each tracking error appears to decrease from one repetition of the doublet to the next. Note that, even without online approximation, the tracking errors of the controller are bounded; however, the bound is significantly larger. The tracking errors for the same initial condition and command sequence, but with the parameter adaptation turned off is shown in Fig. 7; compare with Fig. 5.

Figure 2 shows the initial and final approximations to $C_{M_o}(\boldsymbol{x}_r)$ and $C_{L_o}(\boldsymbol{x}_r) + C_{L_\alpha}(\boldsymbol{x}_r)\alpha$ along with the actual functions. Figure 2 is only shown as a function of α, but the regressor input $\boldsymbol{x}_r$ is multidimensional as described earlier. Note that the approximations converge toward the actual functions for $\alpha \in [3, 10]$, which is the region of the operating envelope about which the vehicle has operated during the duration of this 450-s simulation. Note that convergence of the approximated functions is not required for the tracking errors to behave well. The approximated functions can be forced to converge, if desired, by adding additional excitation (either by changing the γ_c and V_c signals or by altering the actuator signals within the null space of the G matrix).

A. Control Parameter Selection

For selection of the control parameters, consider the nominal tracking error dynamics when the robustifying terms, model error terms, and parametric error terms are all zero. The state-space representation is then

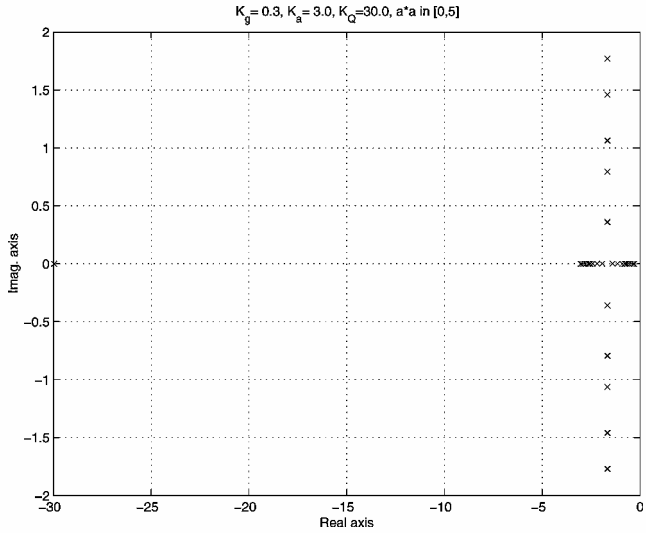

Fig. 8 Root locus for the tracking error dynamics of Eq. (60) as a function of $a^2 \in [0, 5]$ with $K_Q = 30$, $K_\alpha = 3$, and $K_\gamma = 0.3$.

$$\begin{bmatrix} \dot{\tilde{\gamma}} \\ \dot{\tilde{\alpha}} \\ \dot{\tilde{Q}} \end{bmatrix} = \begin{bmatrix} -K_\gamma & a & 0 \\ -a & -K_\alpha & 1 \\ 0 & -1 & -K_Q \end{bmatrix} \begin{bmatrix} \tilde{\gamma} \\ \tilde{\alpha} \\ \tilde{Q} \end{bmatrix} \tag{60}$$

where $a = \bar{q}S\hat{C}_{L_\alpha}/mV$. The poles of this system are determined by the roots of

$$0 = s^3 + (K_\gamma + K_\alpha + K_Q)s^2 + \left(K_\gamma K_\alpha + K_\alpha K_Q + K_Q K_\gamma + a^2 + 1\right)s + \left(K_\gamma K_\alpha K_Q + a^2 K_Q + K_\gamma\right)$$

Although it is not necessary for the theoretical analysis, to achieve timescale separation between the loops, $K_Q > K_\alpha > K_\gamma$ is normal. If this constraint is applied, the error dynamics have one real pole near $-K_Q$ and two poles with a real part in $[-K_\alpha, -K_\gamma]$. For $V \in [200, 900]$ fps, the parameter $a^2 \in [0, 1]$. For the control gains from the example, the root locus as a function of a^2 is shown in Fig. 8. As a^2 increases, these two poles become complex and their damping decreases. Alternatively, the three control gains could be computed online as a function of a^2 to maintain fixed-pole locations.

V. Conclusions

Design, analysis, and simulation results have been presented for a backstepping controller incorporating online approximation of the aerodynamic coefficients as a function over the operating envelope. Several previous results in the literature have presented controllers incorporating online adaptation of linearized aerodynamic coefficients. Because the optimal linearized aerodynamic coefficients change with operating point, such linear adaptive methods may have significant transients when the flight conditions change. Those transients would reoccur as the aircraft cycled through a set of operating points because such linear adaptive approaches are incapable of storing model information as a function of operating point. Online approximation of the aerodynamic coefficients as a function over the operating envelope is a form of spatial memory; each time the aircraft enters a new region of the operating envelope, the model parameters that the controller uses are the last parameters that it had previously estimated while in that region. At the initiation of the controller, prior knowledge about the approximated functions can be used, either by initializing the approximator parameter vectors or by additive known functions. Such prior initialization is not required from a theoretical point of view, but it will improve the initial transient response of the system.

We have presented our approach without explicitly stating an actuator distribution method. The simulation example used

pseudoinverse-based control distribution, but the stability results are not dependent on that actuator distribution approach. Given that various actuator distribution approaches are available, two points are important and will occur with any actuator distribution approach. The first potential issue is that the estimated matrix $\hat{G}_Q$ may lose full row rank even while the actual G_Q matrix still has full row rank. This issue did not occur in our simulation results, but would need to be addressed in a flight-ready control approach. If the designer can define a convex set $\mathcal{S}$, for example, each element of G_Q having an a priori fixed sign, which is known to contain the true control effectiveness parameters and which ensures the full row rank of G_Q, then projection methods can be used to avoid loss of rank of $\hat{G}_Q$. Alternatively, because it is assumed that the actual vehicle is controllable throughout the operating envelope $\mathcal{D}$, it is possible to monitor the condition of $\hat{G}_Q\hat{G}_Q^T$. If this matrix approaches singularity, then the actuator distribution algorithm can use the actuator effectiveness matrix null space to enhance the ability to estimate the actuator effectiveness parameters. The second potential issue is actuator saturation. The actuator distribution algorithm can use the null space of $\hat{G}_Q$ to achieve $\hat{u}_Q$ even though some of the actuators may be at a saturation limit. When it is not possible to achieve $\hat{u}_Q$ due to actuator saturation, nonzero tracking error will occur that is caused by saturation, not by model error; therefore, the online approximation approach will require modification. One approach that will work is to stop the parameter adaptation when $\hat{u}_Q$ is not being achieved due to actuator saturation. A more subtle approach that allows online approximation to continue even during saturation is being developed as a current research project.

The inner-loop control approach can be directly extended to provide a multiaxis (P, Q, R) controller. That extension is not included herein due to space limitations. The outer-loop controller can also be extended to provide (χ, γ, V), (α, β, μ), and (P, Q, R) controllers. That extension is currently being developed.

In the presentation, it was assumed that the regressor $\phi(\boldsymbol{x}_r)$ is defined a priori. Therefore, the model error terms are fixed when the lift, drag, and moment functions are fixed. The fixed regressor assumption is standard in the literature related to online approximation-based control, for example, neural and adaptive fuzzy, for which stability results are desired. Methods that adapt the definition of the regressor vector exist in the literature, for example, Ref. 44, but currently there are no stability results for those approaches. Combining these approaches is also a useful area for future research.

Appendix A: MSS Stability Result

The concept of μ small in the MSS is defined in Ref. 39 as follows.

Definition. Let $x(t): [0, \infty) \mapsto \Re^n$ and $\mu(t): [0, \infty) \mapsto \Re^+$ where $x \in \mathcal{L}_{2e}$ and $\mu \in \mathcal{L}_{1e}$. The signal x is μ small in the MSS if and only if

$$x \in S(\mu) = \left\{ x \,\middle|\, \int_t^{t+T} x(\tau)^T x(\tau)\,\mathrm{d}\tau \le c_0 \int_t^{t+T} \mu(\tau)\,\mathrm{d}\tau + c_1, \forall t \ge 0,\ T \ge 0 \right\}$$

where c_0 and c_1 are finite positive constants. The following theorem will be useful in the main body of the paper.

Theorem A.1: If $|e(t)| \le \bar{e} < \infty, \phi[x(t)] \in \mathcal{L}_\infty$ where $\bar{e}$ is a known positive constant and

$$\dot{\tilde{x}} = -K\tilde{x} - \tilde{\theta}^T\phi + e \qquad \text{for} \qquad K > 0 \tag{A1}$$

$$\dot{\tilde{\theta}} = \begin{cases} 0 & |\tilde{x}| \le \sqrt{2}\bar{e}/K \\ \Gamma\tilde{x}\phi & \text{otherwise} \end{cases} \tag{A2}$$

then $\tilde{x}, \tilde{\theta}, \dot{\tilde{\theta}} \in \mathcal{L}_\infty$; $\tilde{x} \in \mathcal{L}_{2e}$; and $\tilde{x}$ is e^2 small in the MSS.

Proof: Consider the function $\mathcal{V} = \frac{1}{2}(\tilde{x}^2 + \tilde{\theta}\Gamma^{-1}\tilde{\theta})$, which is positive definite with respect to $\tilde{x}$ and $\tilde{\theta}$. The derivative of $\mathcal{V}$ along solutions of Eqs. (A1) and (A2) for $|\tilde{x}| > \sqrt{2}\bar{e}/K$ is

$$\dot{\mathcal{V}} = -K\tilde{x}^2 + e\tilde{x} \tag{A3}$$

When the equality $e\tilde{x} = \frac{1}{2}\{K\tilde{x}^2 + (1/K)e^2 - [\sqrt{K}\tilde{x} - (1/\sqrt{K})e]^2\}$ is used,

$$\dot{\mathcal{V}} \le -(K/2)\tilde{x}^2 + (1/K)|e|^2 \tag{A4}$$

Therefore, if $|\tilde{x}|^2 > 2\bar{e}^2/K^2$, then $\mathcal{V}$ is decreasing. If $|\tilde{x}|^2 \le 2\bar{e}^2/K^2$, then $\tilde{\theta}$ is constant and $|\tilde{x}|$ is bounded. Therefore, $\mathcal{V}(t)$ is bounded by $\mathcal{V}(0)$, which shows that $\tilde{x}, \tilde{\theta} \in \mathcal{L}_\infty$. Because $\phi \in \mathcal{L}_\infty$, Eq. (A2) shows that $\dot{\tilde{\theta}} \in \mathcal{L}_\infty$. Finally, integrating both sides of Eq. (A4) yields

$$\int_t^{t+T} \tilde{x}^2\,\mathrm{d}\tau \le \frac{2}{K}[\mathcal{V}(t) - \mathcal{V}(t+T)] + \frac{2}{K^2}\int_t^{t+T} |e|^2\,\mathrm{d}\tau \le \frac{2}{K}\mathcal{V}(0) + \frac{2}{K^2}\int_t^{t+T} |e|^2\,\mathrm{d}\tau \tag{A5}$$

which shows that $\tilde{x}$ is e^2 small in the MSS, that is, $\tilde{x} \in S(e^2)$.

Appendix B: Reduced Longitudinal Dynamic Model

For $R = P = 0, \phi = 0$, and $\beta = 0$, the aircraft dynamic equations[34] reduce to

$$\dot{V} = (1/m)[T\cos(\alpha) - D - mg\sin(\theta - \alpha)] \tag{B1}$$

$$\dot{\alpha} = (1/mV)[-T\sin(\alpha) - L + mVQ + mg\cos(\theta - \alpha)] \tag{B2}$$

$$\dot{Q} = c_7\bar{M} + f_Q \tag{B3}$$

$$\dot{\theta} = Q \tag{B4}$$

where θ is the pitch angle and the various other symbols are defined in the Nomenclature.

Acknowledgments

This research was supported by Barron Associates, Inc., through U.S. Air Force Contract F33615-01-C-3108, the University of California–Riverside, and the University of Cincinnati.

References

[1] Azam, M., and Singh, S. N., "Invertibility and Trajectory Control for Nonlinear Maneuvers of Aircraft," *Journal of Guidance, Control, and Dynamics*, Vol. 17, No. 1, 1994, pp. 192–200.

[2] Bugajski, D. J., Enns, D. F., and Elgersma, M. R., "A Dynamic Inversion Based Control Law with Application to High Angle of Attack Research Vehicle," *Proceedings of the AIAA Guidance, Navigation, and Control Conference*, AIAA, Washington, DC, 1990, pp. 20–22.

[3] Lane, S. H., and Stengel, R. F., "Flight Control Design Using Nonlinear Inverse Dynamics," *Automatica*, Vol. 31, No. 4, 1988, pp. 781–806.

[4] Menon, P. K. A., Badget, M. E., Walker, R. A., and Duke, E. L., "Nonlinear Flight Test Trajectory Controllers for Aircraft," *Journal of Guidance, Control, and Dynamics*, Vol. 10, No. 1, 1987, pp. 67–72.

[5] Meyer, G., Su, R., and Hunt, L. R., "Application of Nonlinear Transformations to Automatic Flight Control," *Automatica*, Vol. 20, No. 1, 1984, pp. 103–107.

[6] Snell, S. A., Enns, D. F., and Garrard, W. L., "Nonlinear Inversion Flight Control for a Supermaneuverable Aircraft," *Journal of Guidance, Control, and Dynamics*, Vol. 14, No. 4, 1992, pp. 976–984.

[7] Khan, M. A., and Lu, P., "New Technique for Nonlinear Control of Aircraft," *Journal of Guidance, Control, and Dynamics*, Vol. 17, No. 5, 1994, pp. 1055–1060.

[8] Gerrard, W. L., Enns, D. F., and Snell, A., "Nonlinear Longitudinal Control of a Supermaneuverable Aircraft," *Proceedings of the 1989 American Control Conference*, Vol. 1, American Automatic Control Council, 1989, pp. 142–147.

[9] Ward, D., Monaco, J., and Bodson, M., "Development and Flight Testing of a Parameter Identification Algorithm for Reconfigurable Control," *Journal of Guidance, Control, and Dynamics*, Vol. 21, No 6, 1998, pp. 948–956.

[10] Chandler, P. R., Pachter, M., and Mears, M., "System Identification for Adaptive and Reconfigurable Control," *Journal of Guidance, Control, and Dynamics*, Vol. 18, No. 3, 1995, pp. 516–524.

[11] Singh, S. N., and Steinberg, M., "Adaptive Control of Feedback Linearizable Nonlinear Systems with Application to Flight Control," *Journal of Guidance, Control, and Dynamics*, Vol. 19, No. 4, 1996, pp. 871–877.

[12] Steinberg, M. L., and Page, A. B., "Nonlinear Adaptive Flight Control with Genetic Algorithm Design Optimization," *International Journal of Robust and Nonlinear Control*, Vol. 9, 1999, pp. 1097–1115.

[13] Brinker, J. S., and Wise, K. A., "Flight Testing of a Reconfigurable Control Law on the X-36 Tailless Aircraft," *Journal of Guidance, Control, and Dynamics*, Vol. 24, No. 5, 2001, pp. 903–909.

[14] Calise, A. J., Lee, S., and Sharma, M., "Development of a Reconfigurable Flight Control Law for the X-36 Tailless Aircraft," *Journal of Guidance, Control, and Dynamics*, Vol. 24, No. 5, 2001, pp. 896–902.

[15] Rysdyk, R. T., "Adaptive Nonlinear Flight Control," Ph.D. Dissertation, School of Aerospace Engineering, Georgia Inst. of Technology, Atlanta, 1998.

[16] Calise, A. J., and Rysdyk, R. T., "Nonlinear Adaptive Flight Control Using Neural Networks," *IEEE Control Systems Magazine*, Dec. 1998, pp. 14–25.

[17] Steinberg, M. L., "A Comparison of Intelligent, Adaptive, and Nonlinear Flight Laws," *Journal of Guidance, Control, and Dynamics*, Vol. 24, No. 4, 2001, pp. 693–699.

[18] Steinberg, M. L., and Page, A. B., "Automated Recovery System Design with Intelligent and Adaptive Control Approaches," AIAA Paper 2000-4653, 2000.

[19] Steinberg, M. L., and Page, A. B., "A Comparison of Neural, Evolutionary, and Adaptive Approaches for Carrier Landing," AIAA Paper 2001-4085, 2001.

[20] Khalil, H., *Nonlinear Systems*, MacMillan, New York, 1992.

[21] Krstić, M., Kanellakopoulos, I., and Kokotović, P., *Nonlinear and Adaptive Control Design*, Wiley, New York, 1995.

[22] Slotine, J.-J., and Li, W., *Applied Nonlinear Control*, Prentice–Hall, Englewood Cliffs, NJ, 1991, p. 194.

[23] Choi, J. Y., and Farrell, J. A., "Nonlinear Adaptive Control Using Networks of Piecewise Linear Approximators," *IEEE Transactions on Neural Networks*, Vol. 11, No. 2, 2000, pp. 390–401.

[24] Farrell, J. A., "Persistence of Excitation Conditions in Passive Learning Control," *Automatica*, Vol. 33, No. 4, 1997, pp. 699–703.

[25] Farrell, J. A., "Stability and Approximator Convergence in Nonparametric Nonlinear Adaptive Control," *IEEE Transactions on Neural Networks*, Vol. 9, No. 5, 1998, pp. 1008–1020.

[26] Farrell, J. A., "On Performance Evaluation in On-line Approximation for Control," *IEEE Transactions on Neural Networks*, Vol. 9, No. 5, 1998, pp. 1001–1007.

[27] Polycarpou, M. M., "Stable Adaptive Neural Control Scheme for Nonlinear Systems," *IEEE Transactions on Automatic Control*, Vol. 41, No. 3, 1996, pp. 447–451.

[28] Polycarpou, M., and Mears, M., "Stable Adaptive Tracking of Uncertain Systems Using Nonlinearly Parametrized On-Line Approximators," *International Journal of Control*, Vol. 70, No. 3, 1998, pp. 363–384.

[29] Sharma, M., Calise, A. J., and Corban, J. E., "Application of an Adaptive Autopilot Design to a Family of Guided Munitions," AIAA Paper 2000-3969, Aug. 2000.

[30] Trankle, T. L., Vincent, J. H., and Franklin, S. N., "System Identification of Nonlinear Aerodynamic Models," *Advances in the Techniques and Technology of the Application of Nonlinear Filters and Kalman Filters*, AGARDograph No. 256, March 1982.

[31] Batterson, J. G., and Klein, V., "Partitioning of Flight Data for Aerodynamic Modeling of Aircraft at High Angles of Attack," *Journal of Aircraft*, Vol. 26, No. 4, 1989, pp. 334–339.

[32] Iliff, K. W., "Parameter Estimation for Flight Vehicles," *Journal of Guidance*, Vol. 12, No. 5, 1989, pp. 609–622.

[33] Trankle, T. L., and Bachner, S. D., "Identification of a Nonlinear Aerodynamic Model of the F-14 Aircraft," *Journal of Guidance, Control, and Dynamics*, Vol. 18, No. 6, 1995, pp. 1292–1297.

[34] Stevens, B. L., and Lewis, F. L., *Aircraft Control and Simulation*, Wiley, New York, 1992, pp. 80, 88, 131.

[35] Bodson, M., "Evaluation of Optimization Methods for Control Allocation," *Journal of Guidance, Control, and Dynamics*, Vol. 25, No. 4, 2002, pp. 703–711.

[36] Durham, W., "Constrained Control Allocation: Three Moment Problem," *Journal of Guidance, Control, and Dynamics*," Vol. 17, No. 2, 1994, pp. 330–336.

[37] Enns, D., "Control Allocation Approaches," AIAA Paper 98-4109, 1998.

[38] Page, A. B., and Steinberg, M. L., "Closed-Loop Comparison of Control Allocation Methods," AIAA Paper 2000-4538, 2000.

[39] Ioannou, P. A., and Sun, J., *Robust Adaptive Control*, Prentice–Hall, Englewood Cliffs, NJ, 1996.

[40] Polycarpou, M., and Ioannou, P., "A Robust Adaptive Nonlinear Control Design," *Automatica*, Vol. 32, No. 3, 1996, pp. 423–427.

[41] Härkegård, O., and Glad, S. T., "Backstepping Design for Flight Path Angle Control," *Proceedings of the Conference on Decision and Control*, Inst. of Electrical and Electronics Engineers, Piscataway, NJ, 2000, pp. 3570–3575.

[42] Sharma, M., and Ward, D. G., "Flight-Path Angle Control via Neuro-Adaptive Backstepping," AIAA Paper 2002-3520, 2000.

[43] Cox, M. G., "Practical Spline Approximation," *Topics in Numerical Analysis*, Lecture Notes, Vol. 965, Springer-Verlag, Berlin, 1984, pp. 79–111.

[44] Schaal, S., and Atkeson, C. G., "Receptive Field Weighted Regression," ATR Human Information Processing Labs., Technical Rept. TR-H-209, Kyoto, Japan, 1997.